Conceptual Design and Preliminary Analysis of a Fuel-Integrated Energy Recuperating Aircraft Engine

By

Steven Wong

Thesis

Submitted in partial satisfaction of the requirements for the degree of

Master of Science

in

Mechanical and Aerospace Engineering

in the

Office of Graduate Studies

of the

University of California

Davis

Approved:

Paul A. Erickson, Chair

Ralph C. Aldredge

Roger L. Davis

Committee in Charge

2018

Thanks Mom!

Thanks Dad!

Contents

List of Figures

List of Tables

Abstract

Conceptual Design and Preliminary Analysis of a Fuel-Integrated Energy Recuperating Aircraft Engine

A conceptual design for a novel high-bypass turbofan engine was developed and analyzed using fundamental thermodynamic principles. The system is described as having two heat exchangers located between the low and high pressure compressors and after the turbine. The first heat exchanger acts as an intercooler while the second heat exchanger acts as an exhaust recovery system. Air from the core flow passes through the heat exchangers while fuel flows on the other side before entering the combustor. The system reallocates thermal energy generated in the system to preheat the fuel with the desired effect of improving overall efficiency and reducing thrust specific fuel consumption.

If high heat exchanger effectiveness is possible (i.e., $\varepsilon = 0.8$), then such a system can yield a 2.62% reduction in thrust-specific fuel consumption and an increase of 1.44% in overall efficiency and 2.35% in thermal efficiency over a baseline system with identical component efficiencies. If only the intercooler is utilized a higher overall efficiency increase of 2.11% can be achieved although the reduction in thrust-specific fuel consumption lowers to 2.27%.

The effects of multiple major design parameters involved in the design were explored, including heat exchanger effectiveness, pressure drop, and fuel temperature. Based on these effects, practical thresholds for the technology were developed, dictating the design space in which the system is beneficial.

Further work is necessary to actualize the concept including a detailed design for the heat exchangers to establish practical ranges for heat exchanger effectiveness, sizing, and pressure drop as well as a detailed study of fuel thermal and combustion properties.

Acknowledgments

I would be remiss to not acknowledge all those who have carried me through my education at the University of California, Davis.

I acknowledge my advisor, Dr. Paul A. Erickson, who has served as my mentor throughout my undergraduate and graduate education. His guidance through my personal, academic, and professional lives have helped set me on my path to be the engineering scientist that I hope to be.

I acknowledge my committee members, Dr. Ralph C. Aldredge and Dr. Roger L. Davis, who have offered me their invaluable feedback, critique, and time to my work.

I acknowledge my alma mater, the University of California, Davis, and my department, the Department of Mechanical and Aerospace Engineering, which have been the crucibles in which I have refined myself. The faculty, staff, and students here have given me an abundance of resources and support.

I acknowledge my friends and family, both close and distant, who have supported me through troubling times and inspired me to strive for greater things.

I acknowledge my parents, Chou Erl-Shwu and Wong Chung-Hua, whom without which I would have nothing. It is with their endless love, support, and patience that I have anything good in my life. I have only achieved all that I have so far and all that I ever will because of the sacrifices of my parents and the sacrifices of their parents and so on. I hope to continue to make my family proud.

Nomenclature

General

α	bypass ratio
$\dot{m}$	mass flow rate
η	efficiency
γ	ratio of specific heats
π	pressure ratio
τ	temperature ratio
ε	heat exchanger effectiveness
a	speed of sound
c_p	specific heat at constant pressure
c_v	specific heat at constant volume
e	polytropic efficiency
F	thrust
f	fuel-to-air ratio
g_c	Newton's constant
h_{PR}	fuel heating value
HX	heat exchanger
M	Mach number
OPR	overall pressure ratio
P	pressure
R	gas constant
S	uninstalled thrust-specific fuel consumption
T	temperature
TIT	turbine inlet temperature
V	velocity
Nu	Nusselt number

Re	Reynolds number

Subscripts

a	air
b	burner or combustor
c	compressor
d	diffuser or inlet
ER	exhaust recovery (heat exchanger)
f	fan, fuel
fn	fan nozzle
hpc	high pressure compressor
IC	intercooler (heat exchanger)
lpc	low pressure compressor
n	nozzle
O	overall
P	propulsive
T	thermal
t	total, turbine

Chapter 1

Introduction

1.1 Motivation

Innovations in aircraft engines in the past few decades have been driven by the growing demand and necessity to make aircraft more efficient. According to findings from the Environmental Protection Agency (EPA), US aircraft account for around 12 percent of greenhouse gas emissions from transportation and 29 percent of emissions from all aircraft globally [1].

Programs which address these problems have already been initiated in the United States. The Federal Aviation Administration (FAA) NextGen program focuses on the implementation of technologies for the future. This program has made way for the FAA to organize initiatives to achieve a carbon-neutral growth goal for 2020. Additionally, the FAA has awarded $100 million in contracts for the sole purpose of reducing fuel consumption, emissions, and noise through the Continuous Lower Energy, Emissions, and Noise II (CLEEN II) Program. The goal of these programs is to balance environmental protection with sustained aviation growth [2].

There is a clear effort in the United States and globally to produce and implement novel technologies which are more efficient, use less fuel, and produce less emissions. The work presented here aims to follow these goals by providing a preliminary design and analysis for a new technology, a fuel-integrated energy recuperation aircraft engine (FIERA). This high-bypass turbofan engine uses fuel as a thermal reservoir for redistributing heat from

the compressor and turbine to the combustor by preheating the fuel with heat exchangers.

1.2 Background

1.2.1 Gas Turbines and the Brayton Cycle

At the most elementary level, a gas turbine is a power plant which generates power or propulsion through the combustion of fuel in compressed air. The jet engine, shown in Figure 1.1, is a mobile application of the gas turbine.

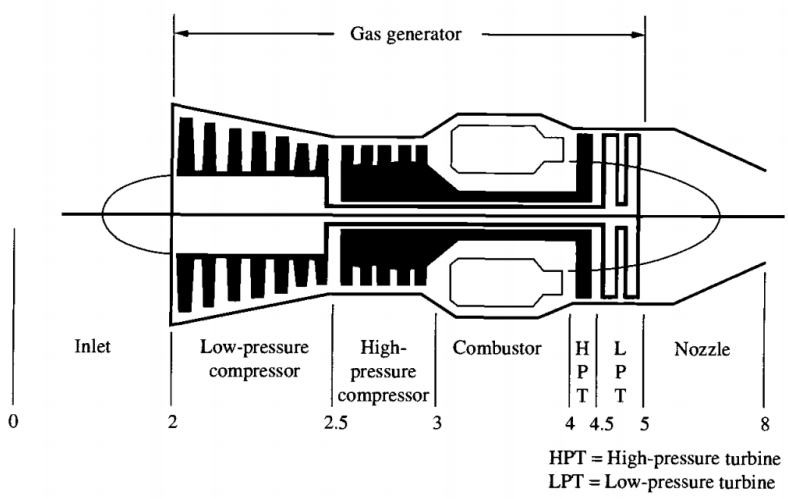

Figure 1.1: The turbojet engine, taken from *Elements of Propulsion* [3].

The fundamental operating principle of the gas turbine is fairly simple from a thermodynamic perspective, following the ideal Brayton cycle shown in Figure 1.2. The station numbering of Figure 1.1 corresponds to the numbering here. Air in the compressor is subjected to isentropic compression. At this higher pressure, the air undergoes isobaric heat addition in the combustor through a combustion process where fuel is added. Now at a higher pressure and temperature, the gas is allowed to expand over a turbine by an isentropic expansion. This generates shaft work.

The cycle shown in Figure 1.2 is an ideal cycle, with efficiency losses neglected. In real applications of the gas turbine, every step has associated losses. This real cycle is shown in Figure 1.3. Note that the expansion and compression stages are now only adiabatic and no longer isentropic.

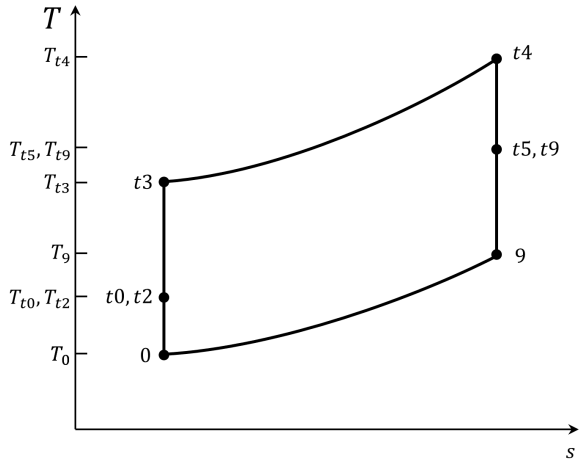

Figure 1.2: The temperature-entropy (T-s) diagram of an ideal turbojet engine.

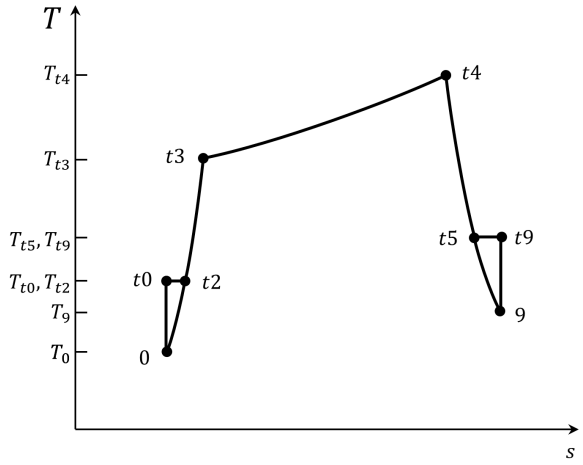

Figure 1.3: The temperature-entropy (T-s) diagram of a real turbojet engine.

1.2.2 Commercial Jet Engines

For most large-scale civilian transport, aircraft are equipped with high-bypass turbofan engines, illustrated in Figure 1.4. This is due to their high efficiencies at subsonic and transonic speeds.

In the high-bypass turbofan engine, thrust is primarily provided by the bypass – around 80% in modern engines – while the gas generator provides the required power. This means that heat can be extracted before the exhaust nozzle without losing a significant amount of thrust.

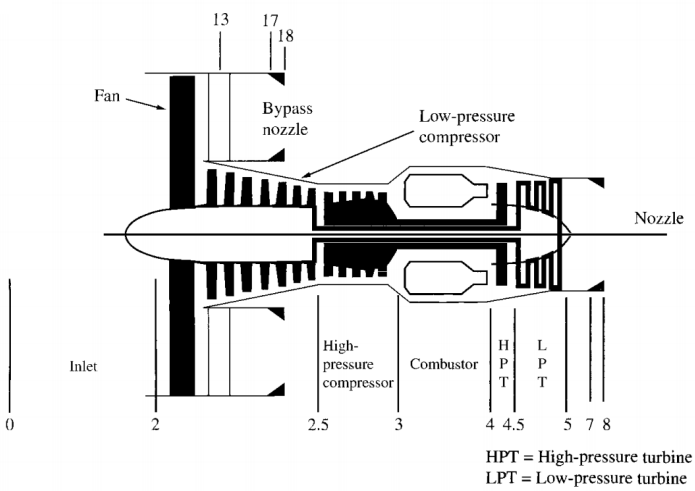

Figure 1.4: The high bypass turbofan, taken from *Elements of Propulsion* [3].

The primary goals of modern commercial jet engines are highest possible thermal and propulsive efficiencies, low jet velocities, and low specific fuel consumption. The consequences of these goals lead to other desired characteristics such as low noise and low emissions. The general approaches which allow for these goals to be met are generally high compressor pressure ratios, high turbine inlet temperatures, and high bypass ratios [3]. However, these are not the only methods by which these goals can be met.

The current most powerful operational high-bypass turbofan engine is the GE-90, although its successor, the GE-9x, is expected to surpass the performance capabilities when it is deployed in 2019. General performance characteristics of the GE-90, as well as those of similar engines are listed here in Table 1.1.

Table 1.1: Details on the GE-90 and other high thrust class turbofan engines [4].

	GE-90	**CF6-80C2**	**RB-211-524G/H**
Company	General Electric	General Electric	Rolls Royce
In use since	Sep 1995	Oct 1985	Feb 1990
Flew on	A-340, B-777	A-300/310, B-747/767	B-747-400/767-300
Weight [kg]	7893	4144	4479
Overall Length [m]	4.775	4.087	3.175
Fan Diameter [m]	3.124	2.362	2.192
Pressure Ratio [-]	39.3	30.4	33
Bypass Ratio [-]	8.4	5.05	4.3
Thrust, cruise [kN]	70	50.4	52.1
SFC [mg/Ns]	8.30	9.32	15.95

1.2.3 Intercooling

Intercooling refers to the process of cooling air flow between the low-pressure and high-pressure compressors. The decreased temperature decreases the power required by the high-pressure compressor. This additionally allows for higher overall pressure ratios if temperatures are a limiting design factor. The T-s diagram for this process, shown in Figure 1.5, illustrates this.

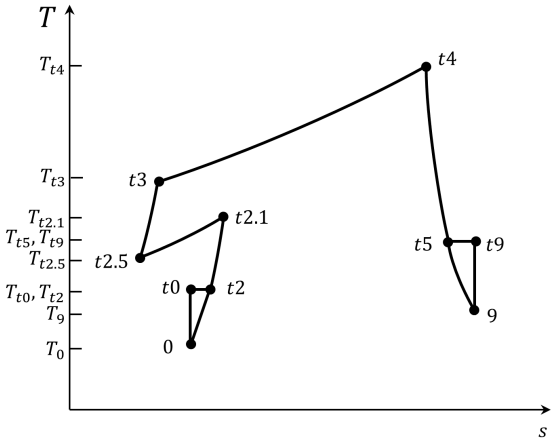

Figure 1.5: Temperature-entropy (T-s) diagram of a turbojet engine with intercooling.

Here it can be seen that the low-pressure compressor brings the air to a maximum temperature after which it is cooled down by transferring heat to the low temperature air from the intercooler. The air is then pressurized again by the high-pressure compressor, which brings it to a maximum temperature again.

1.2.4 Thermal Recovery

Thermal recovery refers to the process of extracting heat from a higher-temperature fluid flow to a lower-temperature fluid flow. This generally involves waste heat in the exhaust air transfered to the air prior to entering the combustor. A distinction between the types of thermal recovery should be made here. Thermal recuperation refers to recovery in which there is no mixing of the different fluids, while thermal regeneration refers to recovery in which there is mixing between the two different temperature fluids.

The basic T-s diagram for this process is shown here in Figure 1.6. Note that in this example, there is 100% recuperative efficiency.

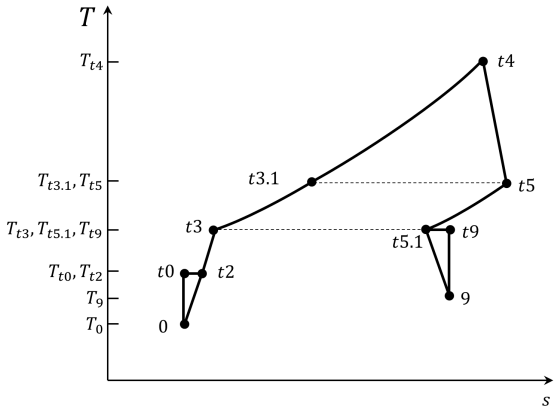

Figure 1.6: Temperature-entropy (T-s) diagram of a turbojet engine with thermal recuperation after the turbine.

Thermal recovery is a common practice in stationary gas turbines as exhaust heat is not typically useful. However, in jet engines used for transportation, a higher temperature exhaust is generally desirable as this allows for higher velocities exiting the nozzle. In the high-bypass turbofan engine, thrust is in large part provided by the bypass, powered by the turbine. This means that heat can be extracted before the core exhaust nozzle

without losing a significant amount of thrust since the lost thrust from the core would be counteracted by the increase in thrust from the bypass [5].

1.2.5 Endothermic Fuels

Endothermic fuels are a class of fuels which can partially break down at high temperatures through an endothermic reaction, thus its namesake. This endothermic reaction can be performed thermally at high temperatures or catalytically at lower temperatures. This reaction absorbs heat and can allow for the effective cooling of components. The heat sink provided by these fuels is a combination of the heating of the fuel and from the endothermic reformation of the fuel.

Endothermic fuels have been proposed for application in supersonic aircraft since the 1960s [9]. High component temperatures necessitate cooling in these vehicles to prevent mechanical failure, making any integrated cooling method desirable for exploration and experimentation. Although still imperative, commercial aircraft do not require the same magnitude of thermal management, so the exploration of these fuels for this application are still limited.

Endothermic fuels could be used as a heat sink for the thermal recuperation processes described above. In traditional thermal recovery systems, the main air flow is used as the cold reservoir. However, endothermic fuels have higher heat capacities, and could also reduce complexity from a design perspective, since the main air stream would not need to be reconfigured for such an application.

The breakdown of the fuel can potentially introduces additional hydrogen into the fuel. This has been shown to improve flame stability, reduce chances of blowout, extend the lean limit of the fuel, and reduce NOx emissions [5].

1.3 Problem Definition

There exists a need for more efficient commercial aircraft engines. Novel and radical concepts for these engines require ample support and development. The first stages of such development are thermodynamic analyses to show that these concepts are worth exploration. In order to predict the benefits of such technology, a conceptual design and

preliminary performance analysis should be made and conducted.

1.4 Research Objectives

The principle goal of this research is to develop a model to illustrate the potential overall benefit of endothermic fuel intercooling and thermal recuperation in high-bypass turbofan engines. This includes an entire conceptual design of this technology applied. A breakdown of this goal and other objectives are listed here.

1. Synthesize research

   The state of thermal management in modern gas turbines should be examined. Initially, this involves a synthesis of research extant in the literature on thermal recovery methods, endothermic fuel properties, and modern turbofan engine technologies. The end goal of this synthesis is a realistic prediction for the system's recuperative efficiency and some insight on what would be necessary in order to improve the efficiency.

2. Develop model for evaluating performance

   A model should be developed akin to the parameterized engine design equations found in Mattingly's *Elements of Gas Turbine Propulsion*, except to include recuperative terms. Performance analysis of this engine should follow, along with iterative design cycles.

3. Identify ideal range for technology to maximize benefits

   The range at which the technology has the greatest impact and benefits should be clearly defined. Design parameters of particular focus are overall pressure ratio, heat exchanger effectiveness, and turbine inlet temperature.

4. Compare to baseline and illustrate enhancement

   The enhancement of performance characteristics from the design should be compared to a baseline, examining changes in overall, thermal, and propulsive efficiencies as well as thrust-specific fuel consumption and other common metrics of aircraft performance.

Chapter 2

Literature Review

The following chapter is a literature review, providing background on the technologies upon which this research depends and similar technologies for context. Included as part of this review is the contribution of this work as it relates to the current body of research.

2.1 Turbine Thermal Management

The primary limitation to higher thermal efficiencies and power outputs of gas turbines for propulsive and power-generation applications is turbine inlet temperature. Outside of an intuitive understanding of gas turbine operation, a theoretical statement of Brayton cycle thermal efficiency makes this obvious, using station numbering from Figure 1.2.

$$\eta_T = 1 - \frac{q_{out}}{q_{in}} = 1 - \frac{c_{pc}(T_9 - T_0)}{c_{pt}(T_{t4} - T_{t3})}$$

Here a higher turbine inlet temperature T_{t4} increases the value of the thermal efficiency η_T. Therefore, much research in gas turbine technology is directed towards enabling a higher value for this temperature. State-of-the-art gas turbines already operate well above the melting point of the blade material (1000°C and 700°C respectively) [6]. This is possible due to advancements in cooling methods. The two primary methods of turbine blade cooling are film cooling and internal cooling, shown here in Figure 2.1. It should be noted however, that although these higher temperatures are desired, some applications which favor lower emissions will aim for lower turbine inlet temperatures to limit thermal NO_x. Even in these cases, maintaining low turbine blade temperatures is still critical.

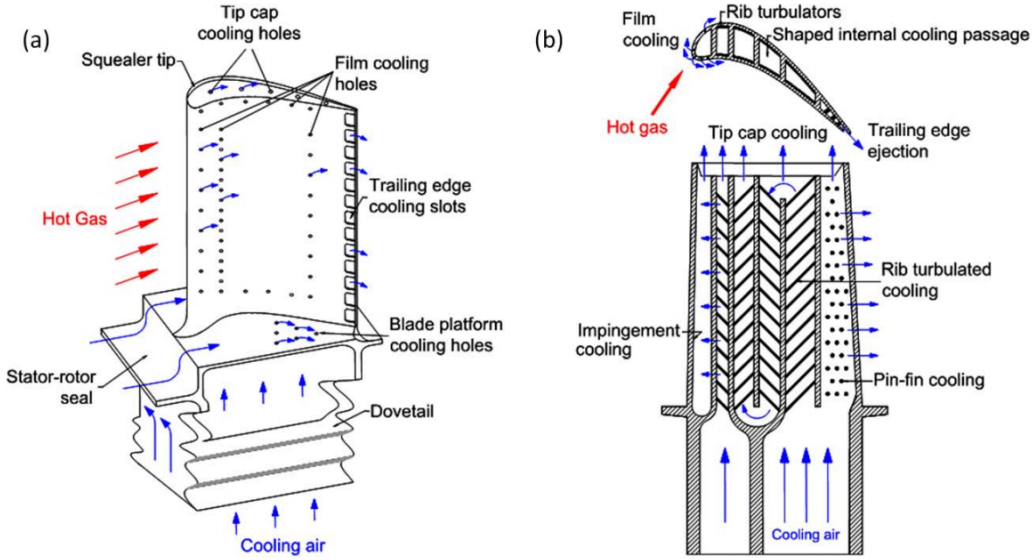

Figure 2.1: Schematic of gas turbine blade cooling with (a) film cooling and (b) internal cooling [7].

2.1.1 Film Cooling

Film cooling, or external cooling, describes a method of cooling by which coolant air is ejected out through holes to provide a protective film which shields the external surface of the blade from hot combustion gases. Since this cooling method utilizes coolant gases, this method is of less relevance to the technology explored in this body of research. However, as it is a primary method of turbine thermal management, some discussion is warranted.

The fundamental concept behind film cooling is fairly simple: relatively cold air typically bled from the compressor is introduced through holes on the turbine blades to form a protective layer. This layer of air absorbs most of the heat load which would otherwise be taken on by the blade material and reintroduces the heat to the main flow. Film cooling performance is dependent upon coolant-to-hot-mainstream pressure ratio, temperature ratio, and the film-cooling-hole geometry, location, configuration, and distribution [6]. The most common locations and configurations are shown in Figure 2.1. In general, higher pressure ratios and lower temperature ratios are desired for maximum cooling. The primary design consideration for such a system is maximizing cooling effect with the least amount of bleed air from the compressor (more of which directly reduces system efficiency).

Since this method of cooling requires coolant to be directly introduced to the mainstream, utilizing a fuel for coolant here would be impractical.

2.1.2 Internal Cooling

Internal cooling describes a method of cooling by which coolant is passed through channels within the turbine blade, convectively removing heat from the blades. This method of cooling is more relevant to this work as it more readily allows for a liquid coolant, although it primarily involves the flow of compressor bleed air much like film cooling.

Channel geometries vary greatly and often are specifically designed for particular blades. To study the fundamental performance differences behind these highly variable channels, research primarily involves square or rectangular channels using aspect ratios (channel width over channel height) to characterize the geometry. Experimental studies have shown that aspect ratio has minimal effect on overall heat transfer enhancement (characterized by $\mathrm{Nu}/\mathrm{Nu}_o$) although pressure losses were minimized with lower aspect ratios, yielding better thermal performance for these geometries [8].

Rib turbulators are structures within internal coolant passages which are designed to trip the boundary layer of the internal flow. This simple function is why they are widely referred to as trip strips." By initiating turbulent flow in the passages, these structures aim to enhance the heat transfer at the cost of a pressure drop penalty. Design parameters of consideration for these structures primarily involve geometry such as rib size, shape, and distribution. Ribs are designed for specific Reynolds numbers and flow attack angle.

Since turbines move at several thousand rotations per minute, rotational effects play a large part in the fluid dynamics of the coolant. Centrifugal and Coriolis forces produce cross-stream secondary flow in the passages. This causes nonuniform heat transfer on otherwise symmetrical geometries, potentially resulting in one side having greatly enhanced heat transfer and the other having greatly reduced heat transfer. This research is very recent and still requires much development due to the engineering challenges of merely creating experimental rigs to study the phenomena.

Heat loads are nonuniform along the cross section of turbine blades, with the leading edge of the blade having the highest heat load, as it is the first section of the physical body

which interacts with the hot flow. This section should therefore have additional cooling to manage the higher load. Impingement cooling is a suitable method of addressing this problem. Impingement cooling involves flowing coolant through small holes, generating a high velocity flow directed at a surface meant to be cooled. This high-velocity jet offers greater convective cooling than the same flow over the surface through a larger entrance area. Design parameters which affect heat transfer for these structures are jet hole size and distribution, jet-to-target surface distance, spent-air cross flow, cooling channel cross section, and the target surface shape.

2.2 Endothermic Hydrocarbon Fuels

As described in Chapter 1, endothermic hydrocarbon fuels refer to fuels which are used as heat sinks because of favorable endothermic reactions that occur at higher temperatures which further augment heat capacity.‘ Studies for these fuels were first conducted in the 1960s, primarily for the application in hypersonic vehicles [9]. This research was driven by the need for heat removal due to the high aerothermal loads from hypersonic flow and combustion. Additionally, combustion characteristics of these heated fuels differ from those at typical operating temperatures. The thermal cracking of fuels has been shown to reduce ignition delay times [10].

Additives can be introduced to extend the heat sink capabilities of fuels. The JP-8 fuel derivative JP-8+100, shown here in Figure 2.2, was first developed with the use of a fuel heat sink in mind [11]. Fairly comparable heat sinks are capable with other modern conventional fuels, with the fuels n-octane and JP-7 having been shown to exhibit similar total heat sinks [12].

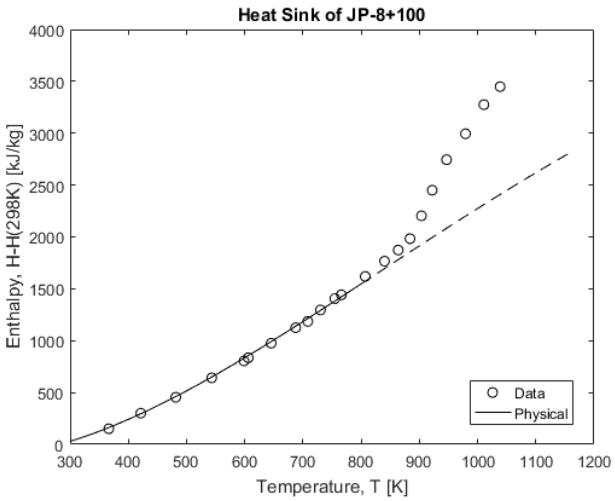

Figure 2.2: Endothermic fuel behavior of JP-8+100, taken from Huang 2002 [12].

More recently, initiator compounds have demonstrated their utility in improving the heat sink capabilities of fuels [13]. The initiator compound used in the study caused JP-7 to produce cracking at lower temperatures and significantly increase the overall fuel heat sink for a given temperature.

2.2.1 Design Considerations and Challenges

A host of design problems surface when endothermic fuels are used. The most prevalent of these problems is carbon deposition, typically referred to as coke formation or coking. As hydrocarbons are heated to high temperatures, carbon forms structures along hot surfaces. Severe buildup of these formations can cause reduced flow rates, increased pressure drops, and ultimately blockage. This phenomenon is the primary setback for fuel heat sinks and other technologies which aim to heat fuels to critical temperatures.

Since this problem is so common and endothermic hydrocarbon fuels have been researched for decades, many solutions have been proposed. These strategies aim to alter either the fuels with additives or the surfaces of the channels which the fuels pass through coatings.

2.2.2 Fuel-Based Heat Exchangers

Given these design considerations and challenges, heat exchangers with fuels require their own specialized design to mitigate undesired effects while maximizing heat transfer for

their specific fluid properties. More conventional design would involve a plate-fin heat exchanger. More recently, a fuel-air metal foam heat exchanger could be used, shown here in Figure 2.3 [12].

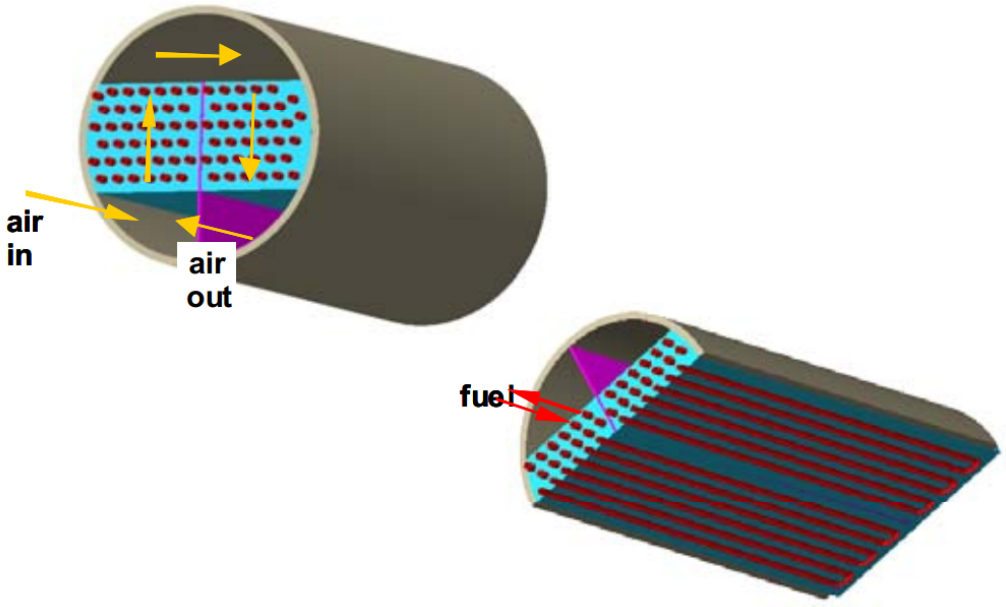

Figure 2.3: Conceptual design of a fuel-air heat exchanger using metal foam, taken from Huang 2002 [12].

2.3 Novel Gas Turbine Concepts

2.3.1 Combined Intercooling and Recuperation

Utilizing both intercooling and recuperation in gas turbines for mobile applications has been practically applied before. The WR-21 Intercooled Recuperated Gas Turbine Engine System (ICR) has been used for marine applications. The primary benefit of the combined intercooling and recuperation is fuel reduction. The intercooler reduces the energy required for the high-pressure compressor while the recuperator improves thermal efficiency and reduces specific fuel consumption by preheating the air prior to entering the combustor with the waste heat from exhaust [14].

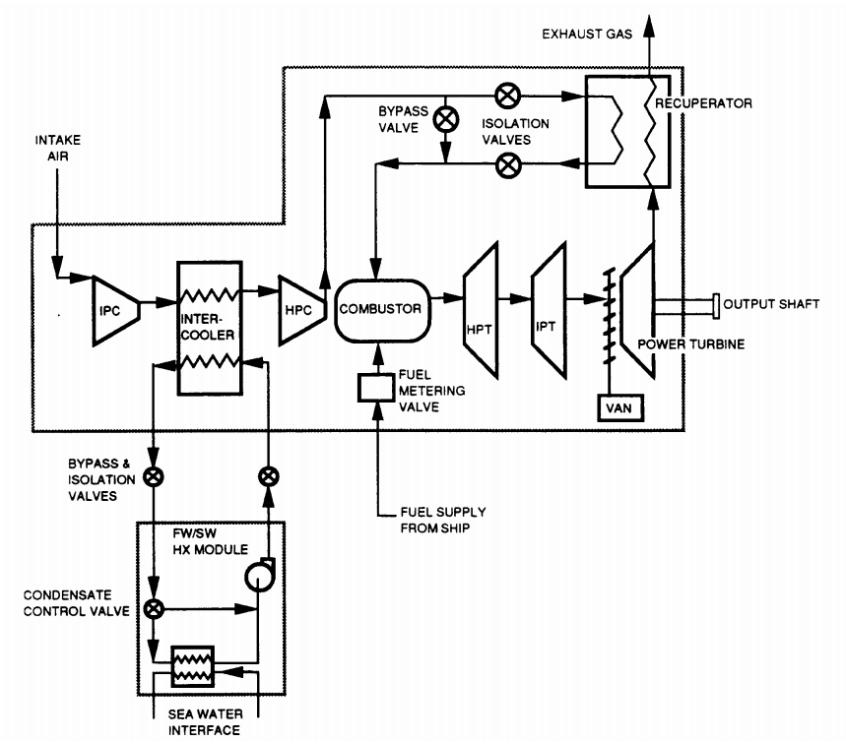

Figure 2.4: Functional operation of intercooled recuperated gas turbine WR21 [14].

In the case of stationary and naval applications, the mechanical complexities of these systems are not of critical concern. The additional weight of heat exchangers and the flow redirection are only minor design considerations which do not play as large of a role in stationary applications. For the application in aircraft, these become major design challenges.

2.3.2 Intercooled Recuperative Aero Engine

A novel system for implementing intercooling and recuperation for an aircraft engine has been in development for a decade by MTU Aero Engines [15]. The intercooled recuperative aero (IRA) engine aims to meet efforts of the European Union through their integrated NEWAC program to design aircraft engines which have higher thermal efficiencies and produce less CO_2 and NO_x emissions. A concept schematic is shown in Figure 2.5, illustrating the functional differences between it and a traditional high-bypass turbofan engine.

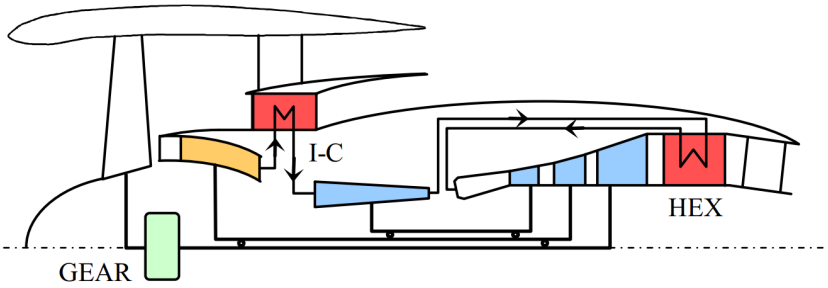

Figure 2.5: Concept schematic of the IRA engine [15].

After the main flow passes through the low-pressure compressor, it is then passed through an intercooler in the bypass flow. This then returns to the high-pressure compressor. This is then lead through to a heat exchanger at the end of the turbine where it collects heat from the flow before it is lead to the nozzle. This heated flow then returns to the combustor where it continues much like a traditional turbofan engine. These components aim to recover thermal energy from the exhaust back into the combustor to ideally reduce the fuel consumption. From a fundamental thermodynamic analysis of the system, it has also been shown to improve thermal efficiency [15, 16].

Since its initial concept phase, more complete mechanical designs and thermofluid modeling have been completed, including advanced component designs. Shown here in Figure 2.6 is a detailed cross section of the IRA engine.

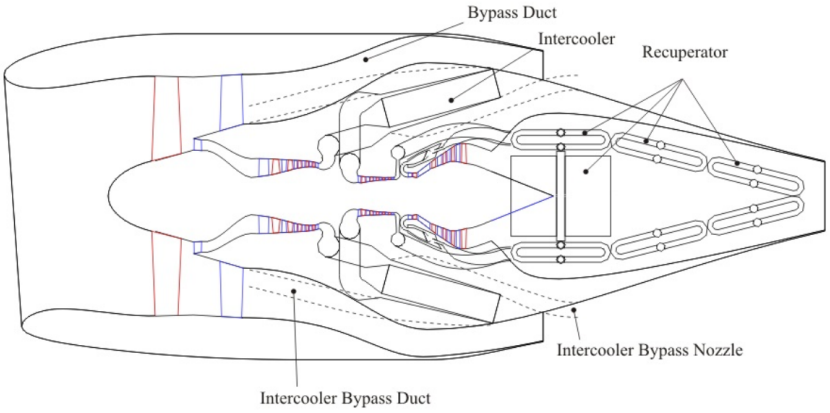

Figure 2.6: Mechanical design and basic component layout of the IRA engine [17].

From first and second law analyses of this system, a net fuel burn reduction ranging from 4.5% to 5.3% is expected depending on the overall pressure ratio [18].

Major challenges still exist in the path to actualizing the concept. Possible failure cases must be studied, leakage remains a considerable concern, and certification for the radical concept could be difficult [17]. However, any new technology which promises large benefits can be expected to have just as many challenges, if not more.

2.3.3 Supercritical CO_2 Bottoming Cycle

Another concept which aims to maximize thermal energy in aircraft engines is the supercritical CO_2 bottoming cycle [19]. This technology has already been shown to be useful for stationary applications, but due to the high power density and efficiency at lower peak cycle temperatures, the benefits could scale for mobile applications.

The system, illustrated in Figure 2.7, uses a supercritical carbon dioxide closed-circuit power cycle to extract heat from the exhaust and utilize it for additional shaft power.

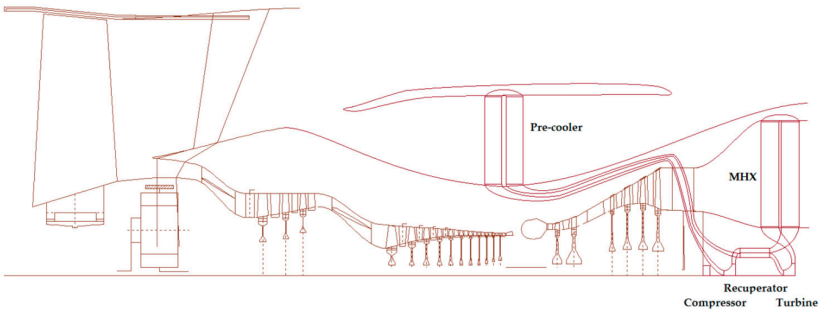

Figure 2.7: Mechanical design and basic component layout of a turbofan engine with a recuperated S-CO_2 bottoming cycle [19].

Here it can be seen that the main heat exchanger is located near the nozzle of the engine. This heats the CO_2, sending the high temperature flow to the bottoming cycle turbine. This work goes directly into the main shaft of the engine. The flow passes through the compressor and then the pre-cooler, which lowers the temperature of the CO_2 using the bypass flow. This then is reintroduced to the main heat exchanger, where the cycle starts again.

Through an initial thermodynamic analysis, this system has an expected 1.9% fuel burn reduction over traditional turbofan engines. As acknowledged by the developers of this system, the desired enhancement for new technologies is closer to a 15% fuel

burn reduction over a reference system. With any new concept, further development is necessary and anything that promises even a modest improvement should be acknowledged and explored.

2.3.4 Turbine Engine with Fuel-Cooled Air Intercooling

An engine design which most closely resembles that presented here is the turbine engine with fuel-cooled air intercooling of US Patent No. 8,220,268 [20]. This patent details a turbine engine design with multiple heat exchangers to extract heat from the main flow between the low and high pressure compressors and as well as from the exhaust, shown here in Figure 2.8.

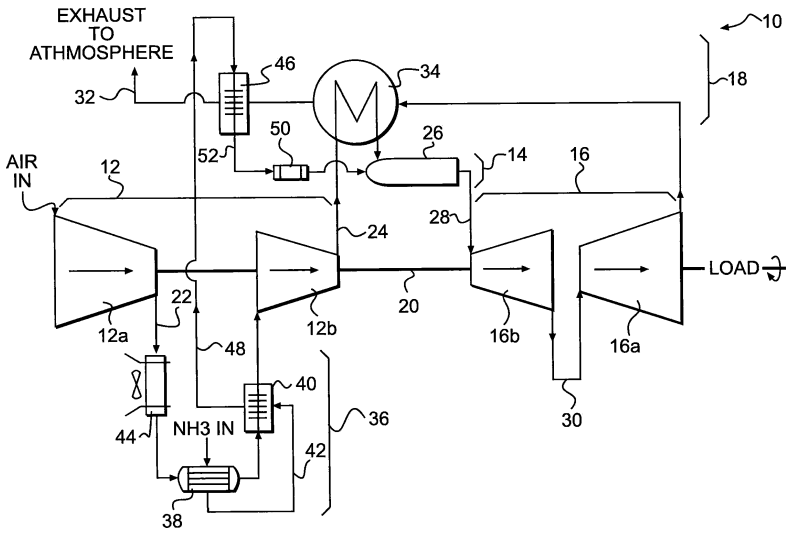

Figure 2.8: Functional diagram of a turbine engine with fuel-cooled air intercooling, presented in US Patent No. 8,220,268 [20].

This patent details a technology particularly different than that which is proposed in the research reported here as it uses an anhydrous ammonia (NH_3) fuel. This has multiple consequences to the overall design of the engine, primarily that the heat exchangers are air-to-air after the initial heating of the fuel in the first heat exchanger of the intercooler. The endothermic hydrocarbon fuel of the technology presented here will most likely remain liquid phase through all the preheat stages, although this must be thoroughly examined in future work. Additionally, this technology aims to extract heat after the compressor

as well, an addition which is clearly not present in the patent.

2.4 Contribution

Radical concepts and configurations are necessary for the advancement of aircraft engine technologies. The work presented here offers a new concept for a commercial turbofan engine configuration along with a fundamental thermodynamic performance analysis to quantify the benefits of such a concept. Detailed in this work is a conceptual design for a high bypass turbofan engine which includes multiple heat exchangers to extract excess thermal energy in the main flow to preheat an endothermic fuel. This study aims to establish a thorough description for the technology, demonstrating potential performance enhancements to a baseline system through a complete fundamental thermodynamic analysis as well as providing guidelines for its further development.

Chapter 3

Approach

3.1 FIERA Concept

The Fuel-Integrated Energy Recuperation Aircraft Engine (FIERA) is a fundamentally simple concept, deviating only slightly from the standard turbofan engine layout. A clear way to describe the engine concept is to follow the path which the fuel takes through the system. Fuel is routed through two heat exchangers as the working fluid which interact with the core air flow, as shown in Figure 3.1.

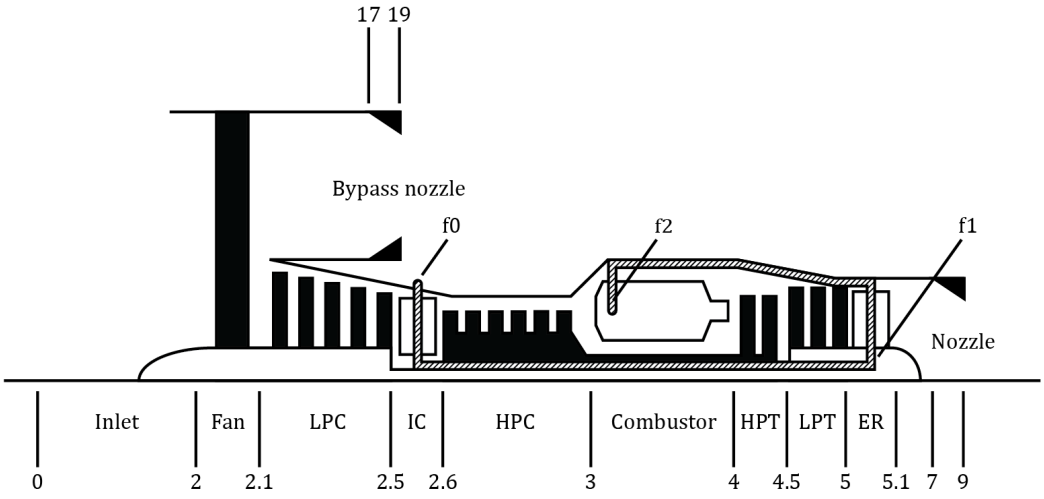

Figure 3.1: Station numbering and component labeling for a fuel-integrated energy recuperation aircraft engine.

Fuel is first directed from storage to the first heat exchanger which acts as an in-

tercooler (IC), lowering the temperature in between the low-pressure and high-pressure compressors in order to increase the maximum achievable pressure ratio. The fuel then flows to the exhaust recovery heat exchanger (ER) which acts to absorb heat from the flow before it enters the nozzle. The fuel then flows to the combustion chamber where it utilizes the energy absorbed throughout the stages.

Table 3.1 shows the station numbering, modified from standard practices described in Aerospace Recommended Practice (ARP) 755 to include the heat exchangers [21].

Table 3.1: Station numbering and description for a fuel-integrated energy recuperation aircraft engine.

Station	Location
0	Far upstream or freestream
1	Inlet/diffuser entry
2	Inlet/diffuser exit, fan entry
2.1	Fan exit, low pressure compressor entry
2.5	Low pressure compressor exit, intercooler entry
2.6	Intercooler exit, high pressure compressor entry
3	High pressure compressor exit, combustor entry
4	Combustor exit, high pressure turbine entry
4.5	High pressure turbine exit, low pressure turbine entry
5	Low pressure turbine exit, exhaust recovery entry
5.1	Exhaust recovery exit
7	Core exhaust nozzle entry
9	Core exhaust nozzle exit
17	Bypass exhaust nozzle entry
19	Bypass exhaust nozzle exit

Table 3.2 shows the various stations of fuel flow. Note that they are numbered in order of the fuel flow and not in order of how they interact with the main flow.

A general T-s diagram for this process would appear as such. Notice that the heat exchanger steps occur in order of increasing temperatures.

Table 3.2: Fuel flow station numbering.

Station	Location
$f0$	Fuel storage exit, intercooler entry
$f1$	Intercooler exit, exhaust recovery entry
$f2$	Exhaust recovery exit, combustor entry

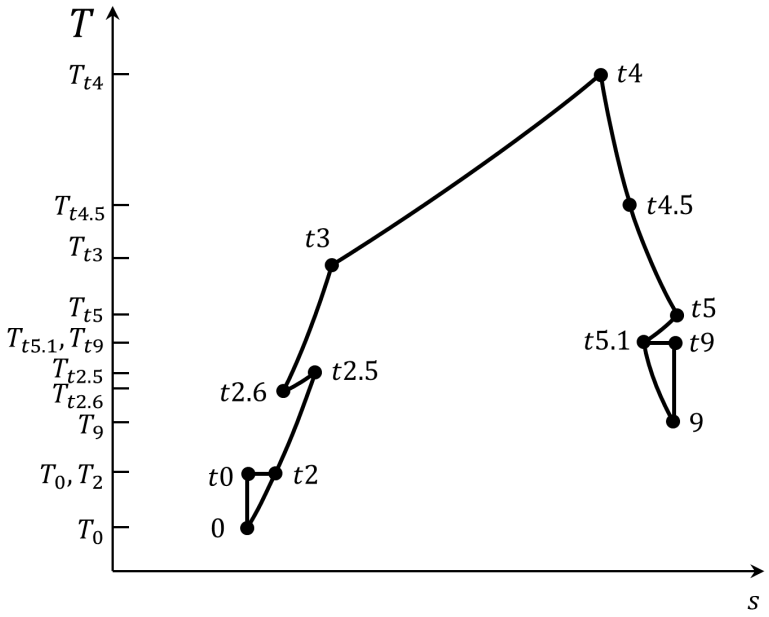

Figure 3.2: The temperature-entropy (T-s) diagram of a fuel-integrated energy recuperation aircraft engine.

3.2 Conceptual Design Procedure

The preliminary design procedure as prescribed by Mattingly's *Aircraft Engine Design* focuses on producing a design fit for a specific size and purpose [22]. This includes design specifications, design point analysis, performance analysis, engine sizing, and component design, iterated for optimization. For the purposes of a fundamental thermodynamic analysis, some of these stages are largely superfluous. Since the focus of this research is to understand the efficiency and performance improvements of the proposed technology, a final design is less important than a thorough understanding of a wide range of parametric values and the enhancement it can provide to a baseline case. As such, the baseline

parameters were selected from a basic set of estimates for a relevant level of technology, listed in Section 3.7.

3.3 Model Approach

The goal of this research is to explore the overall system results and benefits of thermal management and energy recuperation through the use of endothermic fuels.

A parametric model was developed in order to solve for engine characteristics per component. Adapted from equations from Mattingly's *Elements of Propulsion* to include the heat exchangers, this system of equations breaks down components into their pressure ratios, temperature ratios, and efficiencies. This allows for certain terms to be changed and their effects on performance to be identified easily.

The inclusion of the heat exchangers creates the need for two loops in addition to the original set of equations as seen in the model scheme illustrated in Figure 3.3.

The addition of a fuel-based heat exchangers means that the fuel-to-air mass flow rate f, which is typically calculated when solving for the state of the combustor, is needed prior. To do so, an estimate for f is first used for the heat exchanger calculations. Once the calculations all through the combustor and turbine are completed, this new value for f is used. This loop iterates until f stabilizes.

The addition of exhaust recovery means that the state of the flow entering the combustor now depends on the temperature at the exit of the turbine. In order to perform this calculation, another iterative loop must be introduced. First an initial baseline calculation solves for the flow through the combustor and turbine. Then the exhaust recovery heat exchanger properties are solved for, leading back to the combustor and turbine. If the turbine exit conditions in this most recent calculation are not the same as the initial calculation, the code then goes back to recalculate exhaust recovery heat exchanger properties using the latest turbine exit condition. This continues until the calculated turbine exit condition is within an acceptable difference of the previously calculated condition. This loop is nested within the previously described loop.

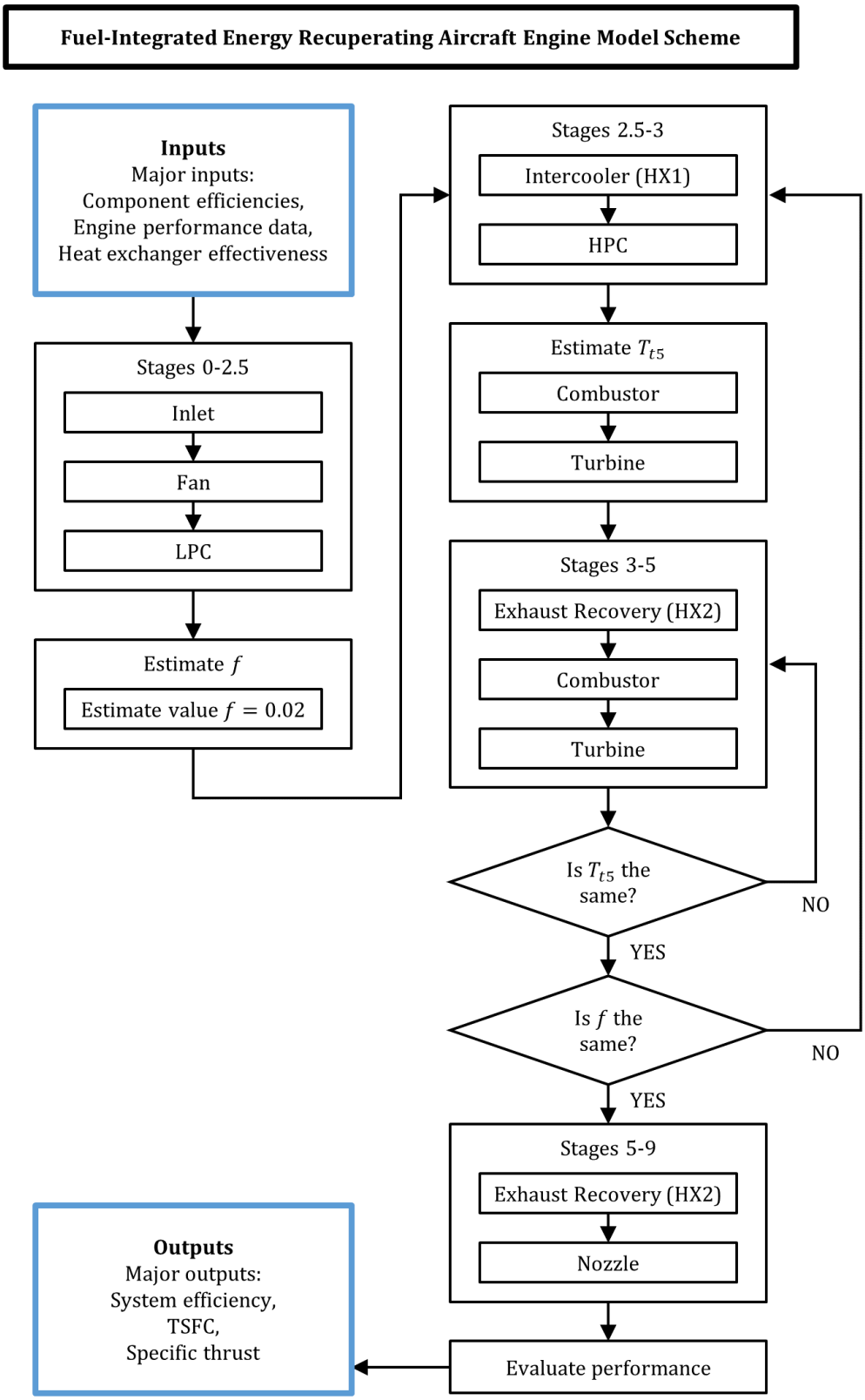

Figure 3.3: General model scheme.

The model then carries out the rest of the parametric system equations, solving for the final performance analysis, evaluating for major characteristics including overall, thermal, and mechanical efficiencies as well as thrust-specific fuel consumption, specific thrust, and others.

3.4 Model Assumptions

The construction of a simple model for a complex system requires a clearly defined set of assumptions. As follows is a list of the assumptions made, primarily based off of those made for the parametric cycle of real engines in Mattingly's *Elements of Gas Turbine Propulsion* [3].

1. The working fluid is air that behaves as a perfect gas with constant properties at different sections: γ_c, R_c, c_{pc} for gas between station 0 and 4; γ_t, R_t, c_{pt} for gas between station 4 and 9.

2. Constant polytropic efficiencies e of compressor, turbine, and fan are used to relate the stage total pressure ratio π to total temperature ratio τ.

3. All components are adiabatic except for the heat exchanger. Heat transfer only occurs in the heat exchangers.

4. Fuel remains unchanged when being transported between heat exchangers and retains all properties from the exit of one heat exchanger to the entry of the next.

3.5 Special Parameters and Functions

Since fuel is used as heat carrier in this system, high temperature variation can be expected throughout. Adjusting fuel thermal properties as a function of temperature is then crucial for reasonable estimates of system performance. As follows are various parameters which must be tracked throughout the system and their temperature dependencies.

3.5.1 Initial Fuel Temperature

The initial fuel temperature ratio is a ratio between the fuel tank temperature and the inlet temperature. Specific details on fuel tank temperatures in commercial aircraft during

cruise were unable to be found. However, based on technical reports and textbooks, it is shown that aircraft fuel tanks generally fluctuate a few degrees from inlet temperatures [23, 24]. Here, the assumption is made that the fuel is stored several degrees above freezing temperatures.

$$T_{f0} = 233\text{K}$$

3.5.2 Fuel Enthalpy

Since the specific heat of fuel c_{pf} is so temperature-dependent, as shown in Figure 3.4, it would be inaccurate to assume constant specific heats across heat exchangers as fuel temperatures are expected to fluctuate greatly. Instead, the enthalpy of the fuel h_f should

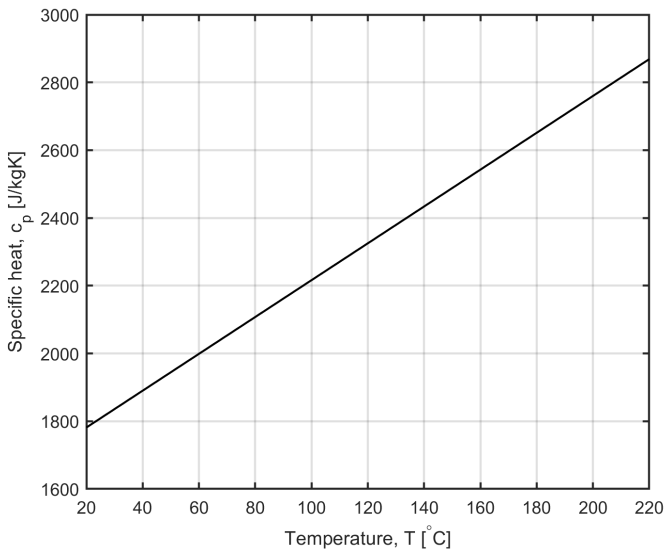

Figure 3.4: Specific heat of JP8 as a function of temperature, taken from *Handbook of Aviation Fuel Properties* [25].

be used to determine changes in the fuel. In addition to being used for calculation of the fuel intercooling and recuperation equations, enthalpy as a function of temperature will be needed for the determination of the heat of combustion of the fuel. A function can be generated from the literature, using data from Huang 2002 presented here in Figure 3.5 [12].

This data is fitted with a piecewise polynomial smoothing spline, to produce the function $h_f(T)$ illustrated here in Figure 3.6a. Additionally, the same technique is applied

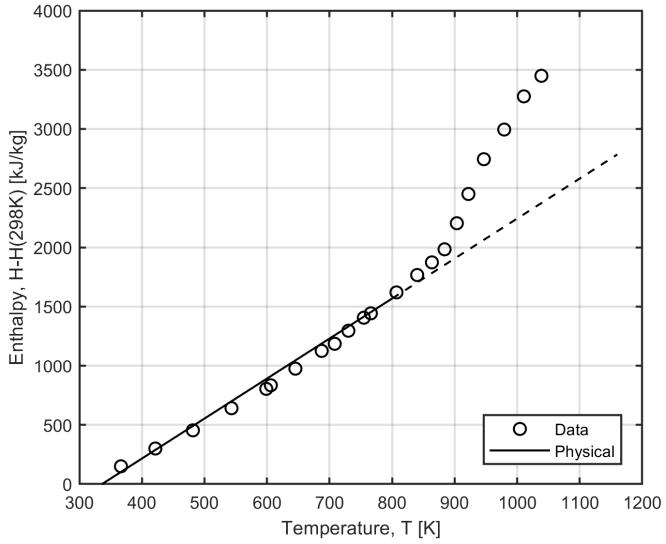

Figure 3.5: Endothermic fuel behavior of JP-8+100, taken from Huang 2002 [12].

to the inverse of the function such that the temperature of the fuel can be calculated given its enthalpy. Presented here in Figure 3.6b is $T_f(h)$.

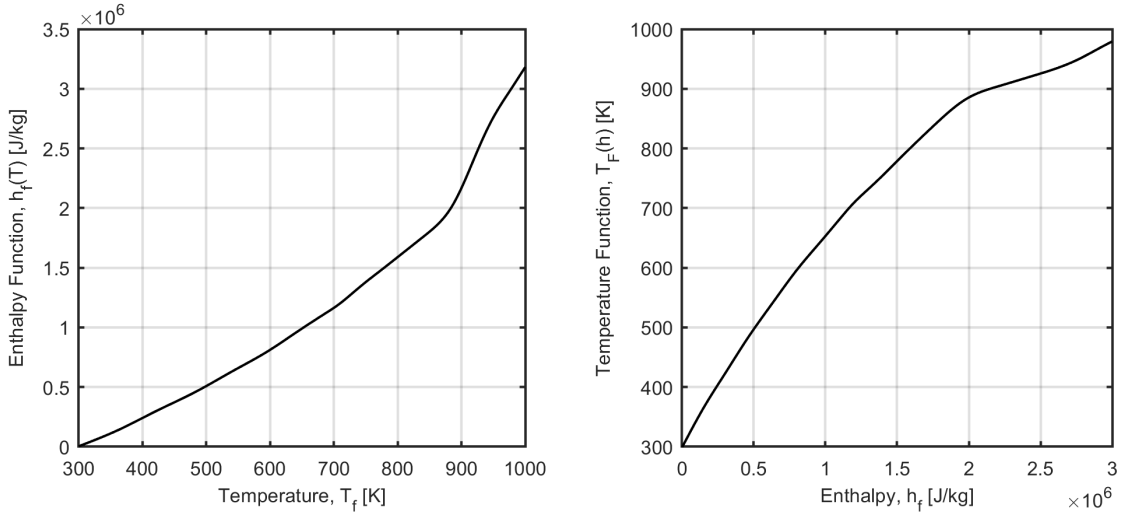

(a) (b)

Figure 3.6: Fuel functions (a) $h_f(T)$, for evaluating the enthalpy of the fuel given its temperature and (b) $T_f(h)$, for evaluating the temperature of the fuel given its enthalpy.

It should be noted that due to the variable specific heat of the fuel, one of the main assumptions typical of the ε-NTU model – that the specific heat of the fluids across the heat exchanger are constant – is not applied here. Here ε is used primarily as a design

parameter to characterize the heat exchanger.

3.5.3 Heat of Combustion

The heat of combustion or enthalpy of combustion h_{PR} of the fuel increases as either the fuel or air temperature increase since the enthalpy of reactants is higher. This fluctuation of the heat of combustion should be accounted for in the energy balance. A higher enthalpy will lower the available heat of combustion, since the reactant enthalpy is higher. The characteristics of the selected fuel JP-8 was drawn directly from the *Handbook of Aviation Fuel Properties* [25].

$$h_{PR} = 43.3 \text{ MJ/kg}$$

If it is assumed that this average enthalpy of combustion is for the fuel at the standard 25°C, then a simple function using the previously determined enthalpy function can be written. Note that the fuel enthalpy function used here has the same reference temperature of 25°C or 298 K.

$$h_{PR}(T) = h_{PR,298\text{K}} + h_f(T)$$

3.5.4 Heat Exchanger Effectiveness

The values for heat exchanger effectiveness ε are dependent on a wide range of factors, including flow stream heat capacity rates, heat capacity rate ratio, and heat exchanger geometry. Without modeling the geometry and materials of the heat exchangers, an accurate value cannot be calculated. Instead, some prediction should be made at a reasonable value for effectiveness.

Figure 3.7 here shows the effectiveness of a single pass, cross-flow heat exchanger with unmixed fluids. This represents the most probable layout for the heat exchanger used in this application.

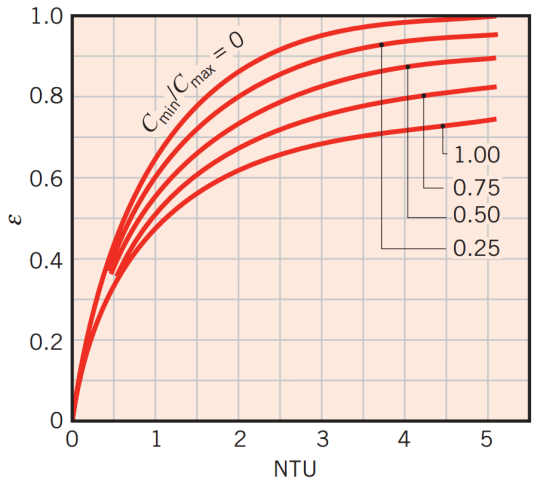

Figure 3.7: Effectiveness for a single-pass, cross-flow heat exchanger with both fluids unmixed, taken from *Fundamentals of Heat and Mass Transfer* [26].

To estimate C_{min}/C_{max} at the first heat exchanger, a high estimate for fuel-to-air ratio of $f = 0.02$ can be used along with specific heat data pulled from Figure 3.4.

$$\begin{aligned}
\frac{C_{min}}{C_{max}} &= \frac{\dot{m}_f c_{pf}}{\dot{m}_a c_{pc}} \\
&= \frac{f c_{pf}}{c_{pc}} \\
&= \frac{(0.02)\left(1800 \frac{\text{J}}{\text{kgK}}\right)}{\left(1004 \frac{\text{J}}{\text{kgK}}\right)} \\
\frac{C_{min}}{C_{max}} &= 0.0359
\end{aligned}$$

Given the low value for C_{min}/C_{max}, higher effectivenesses should be easier to achieve than if the ratio were higher. Here it is assumed that high values for NTU are possible and make a generous estimate for the upper limit of effectiveness.

$$\varepsilon_{max} = 0.80$$

3.5.5 Heat Exchanger Pressure Drop

Flow through heat exchangers experience a pressure drop. Much like with effectiveness, without a clear design, it is difficult to accurately estimate the exact pressure drop on

both sides. Here it is assumed that a modest pressure drop of 1% occurs. A wide range of values for pressure drop should be tested in order to evaluate system viability.

$$\pi_{HX} = 0.99$$

3.6 Model Equation Derivations

As mentioned previously, most equations used have been adapted from Mattingly's *Elements of Propulsion* and El-Sayed's *Aircraft Propulsion and Gas Turbine Engines* [3, 4]. Exceptions to these equations are described in detail here with derivations.

3.6.1 Intercooler

Typical aircraft and industrial gas turbines with intercooling utilize air for the cooling flow. This makes for a simpler formulation of the heat transfer between the two fluids. In the case of fuel as the cold flow, a slightly different set of equations must be written due to the differing specific heats of the air and fuel. As follows is the formulation for these equations.

$$\varepsilon_{MC} = \frac{c_{pc}\dot{m}_a(T_{t2.5} - T_{t2.6})}{\dot{m}_f\,(h_f(T_{t2.5}) - h_{f0})}$$

Using the variable for fuel-to-air mass flow rate f, the equation simplifies slightly.

$$\varepsilon_{MC} = \frac{c_{pc}(T_{t2.5} - T_{t2.6})}{f(h_f(T_{t2.5}) - h_{f0})}$$

This statement can be rearranged to yield an equation for the temperature of the main flow leaving the intercooler.

$$\varepsilon_{MC} f(h_f(T_{t2.5}) - h_{f0}) = c_{pc}(T_{t2.5} - T_{t2.6})$$

$$\boxed{T_{t2.6} = T_{t2.5} - \frac{\varepsilon_{MC} f}{c_{pc}}(h_f(T_{t2.5}) - h_{f0})}$$

Similarly, to get the state of the fuel leaving the intercooler at $f1$, a statement regarding the heat exchange between the two reservoirs can be used since the temperature of the

main flow leaving the intercooler is now known.

$$c_{pc}\dot{m}_a(T_{t2.5} - T_{t2.6}) = \dot{m}_f(h_{f1} - h_{f0})$$

$$c_{pc}(T_{t2.5} - T_{t2.6}) = f(h_{f1} - h_{f0})$$

$$\boxed{h_{f1} = h_{f0} + \frac{c_{pc}}{f}(T_{t2.5} - T_{t2.6})}$$

The fuel temperature function $T_f(h)$ can be used to find the temperature of the fuel at this stage, although the further calculations of later stages do not require this calculation. Thus, leaving it simply as enthalpy is sufficient. This is true for the calculations regarding the other heat exchangers.

3.6.2 Exhaust Recovery

Derivation of the exhaust recovery heat exchanger equations starts with the effectiveness of this heat exchanger ε_{PT}. This follows the same derivation as the equations regarding the intercooler. Presented first is the equation for the main flow exiting the extractor.

$$\varepsilon_{PT} = \frac{c_{pt}(\dot{m}_a + \dot{m}_f)(T_{t5} - T_{t5.1})}{(\dot{m}_f)(h_f(T_{t5}) - h_{f1})}$$

$$\varepsilon_{PT} = \frac{c_{pt}(1+f)(T_{t5} - T_{t5.1})}{f(h_f(T_{t5}) - h_{f1})}$$

$$\varepsilon_{PT} f(h_f(T_{t5}) - h_{f1}) = c_{ot}(1+f)(T_{t5} - T_{t5.1})$$

$$\boxed{T_{t5.1} = T_{t5} - \frac{\varepsilon_{PT} f}{c_{pt}(1+f)}(h_f(T_{t5}) - h_{f1})}$$

An equation can be written for the enthalpy of the fuel leaving this heat exchanger without having the term for $T_{t5.1}$ as this makes more sense for the series of calculations.

$$\varepsilon_{PT} = \frac{\dot{m}_f(h_{f2} - h_{f1})}{\dot{m}_f(h_f(T_{t5}) - h_{f1})}$$

$$\varepsilon_{PT} = \frac{h_{f2} - h_{f1}}{h_f(T_{t5}) - h_{f1}}$$

$$\boxed{h_{f2} = h_{f1} + \varepsilon_{PT}(h_f(T_{t5}) - h_{f1})}$$

3.7 Baseline Parameters

Other parameters not previously described have to be established as well. As follows are baseline parameters from published characteristics of the GE-90 as well as estimates from

technology level D as described in Mattingly's *Aircraft Engine Design* [22]. These values largely represent achievable limits rather than the actual design point.

Table 3.3: Input parameters and data for baseline high bypass turbofan engine.

Term	Value	Term	Value
M_0	0.85	π_n	0.98
T_0 [K]	218.934	π_{fn}	0.99
γ_c	1.4	e_c	0.91
c_{pc} [J/kgK]	1004	e_f	0.93
γ_t	1.35	e_t	0.93
c_{pt} [J/kgK]	1096	η_b	0.99
h_{PR} [J/kg]	4.80e7	η_m	0.99
π_d	0.99	P_0/P_9	0.9
π_f	1.7	P_0/P_{19}	0.9
π_{lpc}	4.85	TIT [°K]	1380
π_{hpc}	4.85	α	7.0
π_b	0.98		

For some parameters, these values were varied over a range in order to evaluate their impact on performance values. A final design configuration and parameters are given in Chapter 4.

3.8 Model Equations

As stated previously, the model relies primarily on the parametric model from Mattingly's *Elements of Propulsion* and El-Sayed's *Aircraft Propulsion and Gas Turbine Engines*, altered to include intercooling and recuperation terms [3, 4].

3.8.1 Stages 0-2.5

Coefficients

$$R_c = \frac{\gamma_c - 1}{\gamma_c} c_{pc}$$
$$R_t = \frac{\gamma_t - 1}{\gamma_t} c_{pt}$$

Inlet

$$a_0 = \sqrt{\gamma_c R_c g_c T_0}$$
$$V_0 = a_0 M_0$$
$$P_{t0} = \left(1 + \frac{\gamma_c - 1}{2} M_0^2\right)^{\gamma_c/(\gamma_c - 1)} P_0$$
$$T_{t0} = \left(1 + \frac{\gamma_c - 1}{2} M_0^2\right) T_0$$
$$P_{t2} = \pi_d P_{t0}$$
$$T_{t2} = T_{t0}$$

Fan

$$P_{t2.1} = \pi_f P_{t2}$$
$$T_{t2.1} = \pi_f^{(\gamma_c - 1)/(\gamma_c e_f)} T_{t2}$$

Low Pressure Compressor (LPC)

$$P_{t2.5} = \pi_{lpc} P_{t2.1}$$
$$T_{t2.5} = \pi_{lpc}^{(\gamma_c - 1)/(\gamma_c e_c)} T_{t2.1}$$

3.8.2 Estimate and Iterate f

Initial Guess and Iterative Looping Condition (Loop goes from Stage 2.5 to 5)

$$f_{new} = 0$$
$$dx = |f_{new} - f|$$
$$\text{while } dx > 0.0001$$

3.8.3 Stages 2.5-3

Intercooler

$$P_{t2.6} = \pi_{MC} P_{t2.5}$$

$$T_{t2.6} = T_{t2.5} - \frac{\varepsilon_{MC} f}{c_{pc}} (h_f(T_{t2.5}) - h_{f0})$$

$$h_{f1} = h_{f0} + \frac{c_{pc}}{f} (T_{t2.5} - T_{t2.6})$$

High Pressure Compressor (HPC)

$$P_{t3} = \pi_{hpc} P_{t2.6}$$

$$T_{t3} = \pi_{hpc}^{(\gamma_c - 1)/(\gamma_c e_c)} T_{t2.6}$$

3.8.4 Estimate and Iterate T_{t5}

Combustor

$$P_{t4} = \pi_b P_{t3}$$

$$T_{t4} = \text{TIT}$$

$$h_{PR} = h_{PR,298\text{K}}$$

$$f = \frac{c_{pt} T_{t4} - c_{pc} T_{t3}}{\eta_b h_{PR} - c_{pt} T_{t4}}$$

Turbine

$$T_{t5new} = \left(1 - \left(\frac{c_{pc} T_{t0}}{\eta_m (1+f) c_{pt} T_{t4}}\right) \left(\frac{T_{t3}}{T_{t2}} - 1 + \alpha \left(\frac{T_{t2.1}}{T_{t2}} - 1\right)\right)\right) T_{t4}$$

Initial Guess and Iterative Looping Condition (Loop goes through Stages 3 to 5)

$$T_{t5new} = 0$$

$$dy = |T_{t5new} - T_{t5}|$$

$$\text{while } dy > 0.0001$$

3.8.5 Stages 3-5

Exhaust Recovery

$$h_{f2} = h_{f1} + \varepsilon_{PT} (h_f(T_{t5}) - h_{f1})$$

Fuel

$$h_{PR} = h_{PR,298\text{K}} + h_{f2}$$

Combustor

$$P_{t4} = \pi_b P_{t3}$$

$$T_{t4} = \text{TIT}$$

$$f_{new} = \frac{c_{pt} T_{t4} - c_{pc} T_{t3}}{\eta_b h_{PR} - c_{pt} T_{t4}}$$

Turbine

$$T_{t5new} = \left(1 - \left(\frac{c_{pc} T_{t0}}{\eta_m (1 + f_{new}) c_{pt} T_{t4}}\right)\left(\frac{T_{t3}}{T_{t2}} - 1 + \alpha\left(\frac{T_{t2.1}}{T_{t2}} - 1\right)\right)\right) T_{t4}$$

3.8.6 Stages 5-9

Turbine

$$f = f_{new}$$

$$T_{t5} = T_{t5new}$$

$$P_{t5} = \left(\frac{T_{t5}}{T_{t4}}\right)^{\gamma_t/((\gamma_t - 1)e_t)} P_{t4}$$

Exhaust Recovery

$$T_{t5.1} = T_{t5} - \frac{\varepsilon_{PT} f}{c_{pt}(1 + f)}(h_f(T_{t5}) - h_{f1})$$

$$P_{t5.1} = \pi_{PT} P_{t5}$$

Nozzle

$$P_{t9} = \pi_n P_{t5.1}$$

$$P_9 = \frac{P_0}{P_0/P_9}$$

$$M_9 = \sqrt{\left(\frac{2}{\gamma_t - 1}\right)\left(\left(\frac{P_{t9}}{P_9}\right)^{(\gamma_t - 1)/\gamma_t} - 1\right)}$$

$$T_9 = T_{t5.1}\left(\frac{P_{t9}}{P_9}\right)^{(1-\gamma_t)/\gamma_t}$$

$$T_9/T_0 = \frac{T_9}{T_0}$$

$$V_9/a_0 = M_9\sqrt{\frac{\gamma_t R_t T_9/T_0}{\gamma_c R_c}}$$

Fan Nozzle

$$P_{t19} = \pi_{fn} P_{t2.1}$$

$$P_{19} = \frac{P_0}{P_0/P_{19}}$$

$$M_{19} = \sqrt{\left(\frac{2}{\gamma_c - 1}\right)\left(\left(\frac{P_{t19}}{P_{19}}\right)^{(\gamma_c - 1)/\gamma_c} - 1\right)}$$

$$T_{19} = T_{t2.1}\left(\frac{P_{t19}}{P_{19}}\right)^{(1-\gamma_c)/\gamma_c}$$

$$T_{19}/T_0 = \frac{T_{19}}{T_0}$$

$$V_{19}/a_0 = M_{19}\sqrt{T_{19}/T_0}$$

3.8.7 Performance

$$F/\dot{m} = \frac{1}{1+\alpha}\frac{a_0}{g_c}(1+f)V_9/a_0 - M_0 + (1+f)\left(\frac{R_t T_9/T_0}{R_c V_9/a_0}\right)\left(\frac{1 - P_0/P_9}{\gamma_c}\right) + \frac{\alpha}{1+\alpha}\frac{a_0}{g_c}\left(V_{19}/a_0 - M_0 + \frac{T_1 9/T_0}{V_1 9/a_0}\frac{1 - P_0/P_{19}}{\gamma_c}\right)$$

$$S = \frac{f}{(1+\alpha)F/\dot{m}}$$

$$\eta_T = \frac{a_0^2(1+f)(V_9/a_0)^2 + \alpha(V_{19}/a_0)^2 - (1+\alpha)M_0^2}{2g_c f h_{PR}}$$

$$\eta_P = \frac{2M_0\left((1+f)V_9/a_0 + \alpha V_{19}/a_0 - (1+\alpha)M_0\right)}{(1+f)(V_{19}/a_0)^2 - (1-\alpha)M_0^2}$$

$$\eta_O = \eta_P \eta_T$$

Chapter 4

Results and Discussion

4.1 Performance

Before exploring the effects of different design parameters, it should first be established which arrangements of heat exchangers provide the greatest benefit to overall performance. This requires comparing multiple configurations over a range of parameters. When a heat exchanger is not present, the code simply assumes the effectiveness of that heat exchanger is $\varepsilon = 0$ and the pressure ratio across it is $\pi_{HX} = 1$ (i.e., no pressure drop).

4.1.1 Efficiency

The limits of the technology are first presented in Figure 4.1 by illustrating the overall efficiencies of the possible heat exchanger configurations over a range of overall pressure ratios. The difference from the baseline layout of no heat exchangers should be examined as well, presented in Figure 4.2. Note that although this value is a percentage, it is not a percent change or difference but rather the difference between two percentages.

From Figure 4.2, it can be seen that the greatest efficiency enhancement is provided by the configuration with the intercooler only (red line). Configuration with both heat exchangers (teal line) also has considerable performance at higher pressure ratios even though it hinders efficiency at pressure ratios under $OPR = 20$.

It is also important to consider the enhancement in Figure 4.2 in context of the raw values presented in Figure 4.1. From just the enhancement alone it appears as if the inclusion of heat exchangers would be most beneficial at the highest achievable pressure ratios.

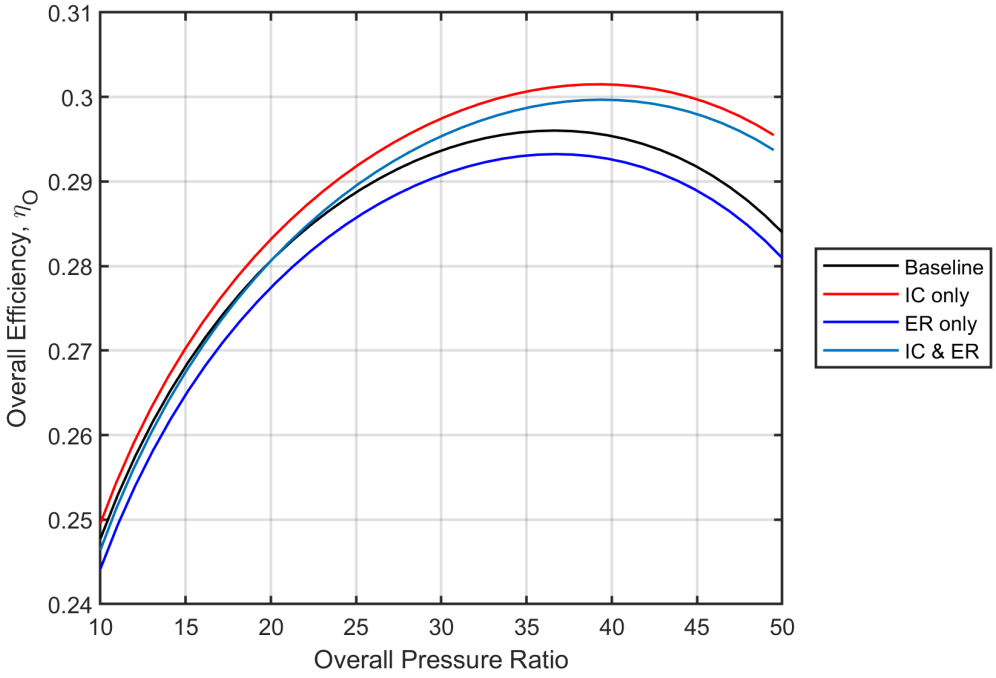

Figure 4.1: Overall efficiency η_O plotted against compressor pressure ratio π_c for all heat exchanger configurations.

However, when looking at values in Figure 4.1, it can be seen that the rate of increase in enhancement is mostly due to the drop-off in overall efficiency in the baseline case after the maximum at $OPR = 36$. The maximum overall efficiency for the best-case configuration occurs at $OPR = 40$. Based on this result, these configurations essentially extend the viable range of pressure ratios for a given set of input parameters while additionally increasing the maximum achievable efficiency.

Since overall efficiency is defined as the product between propulsive and thermal efficiencies, it is important to investigate these two terms separately to identify why the overall efficiency behaves the way it does.

Comparing propulsive efficiencies first in Figure 4.3, the most notable difference between this plot and that of the overall efficiencies is that the configuration without an intercooler (blue line) has a higher propulsive efficiency than those with one (red and teal lines). This would imply that the opposite is true for thermal efficiency, with these benefits being much greater, confirmed by Figure 4.4. Comparing these two figures, the

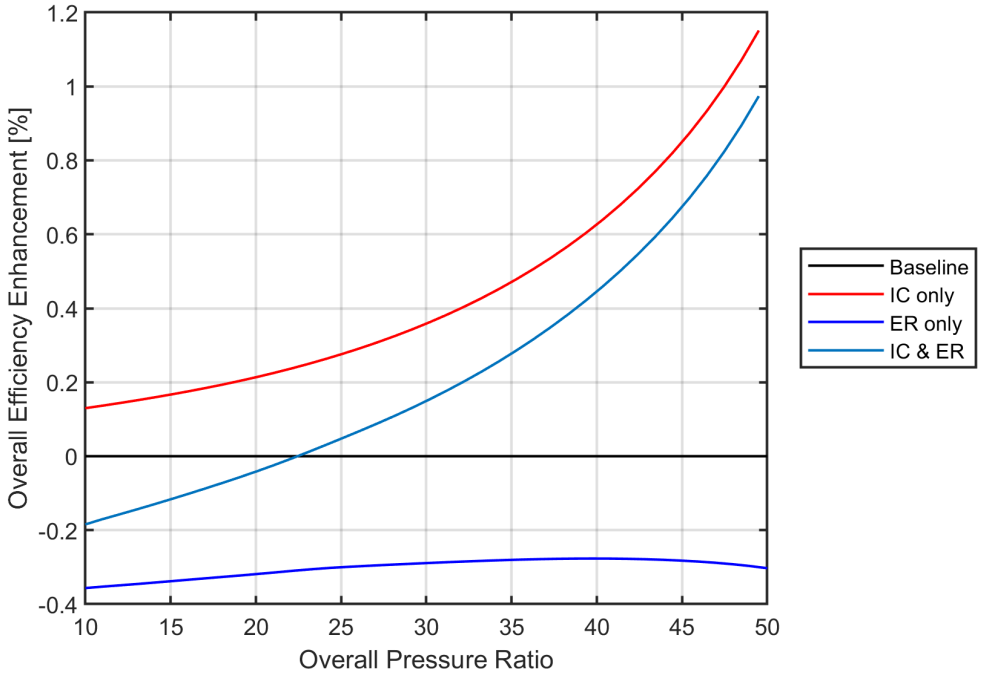

Figure 4.2: Percentage change in overall efficiency η_O plotted against compressor pressure ratio π_c for all heat exchanger configurations.

order in which these lines appear is reversed. The system offers a benefit in thermal efficiency at the cost of propulsive efficiency as it utilizes energy that would be converted to propulsion in the hot jet as thermal energy to be extracted by the turbine.

The intercooler appears to have a net positive effect on overall efficiency, while the exhaust recovery heat exchanger appears to have a negative effect. These results were expected, as pulling heat from the compressor serves to reduce back work on the turbine, generating an overall increase in efficiency. The benefits of exhaust recovery come at a trade-off for aircraft engines since the energy of the exhaust is still utilized to produced thrust. Instead the benefits manifest in lower fuel consumption, which can possibly make up for this loss in overall efficiency.

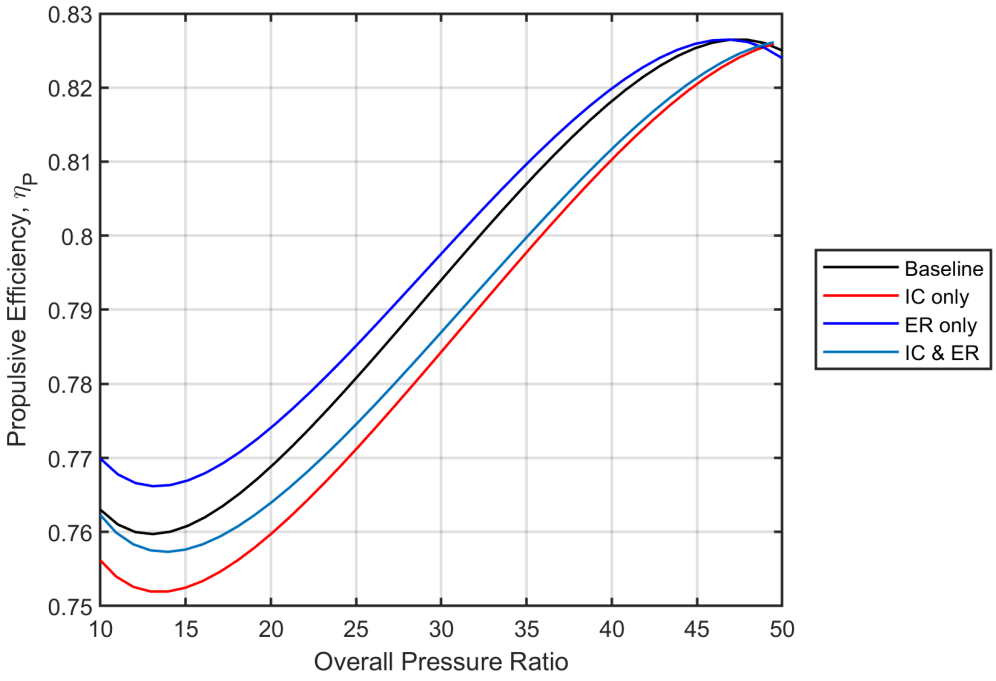

Figure 4.3: Propulsive efficiency η_P plotted against compressor pressure ratio π_c for all heat exchanger configurations.

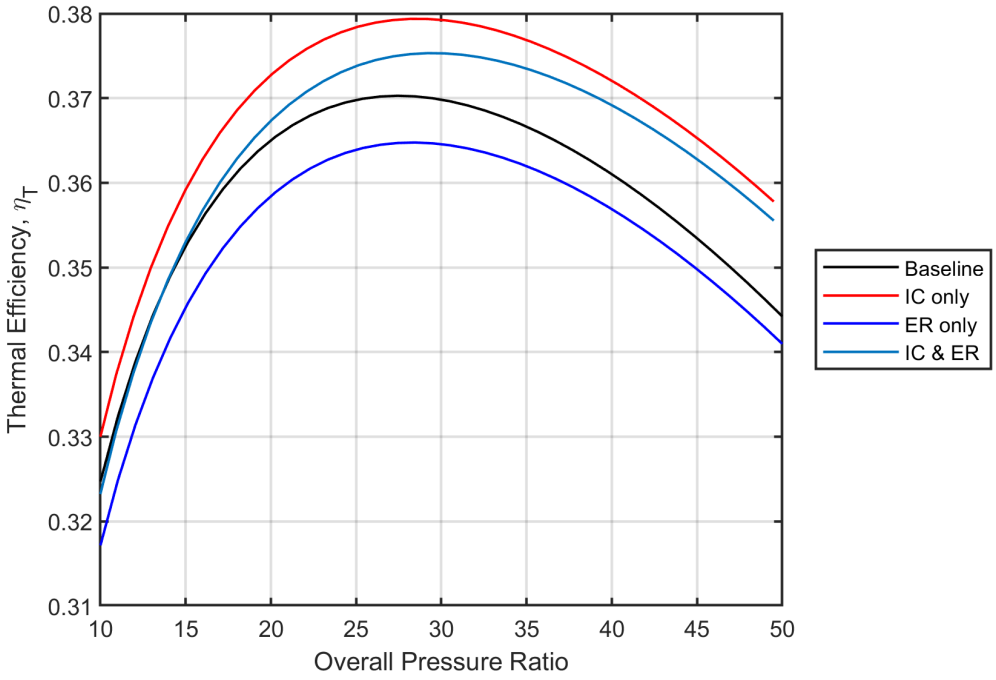

Figure 4.4: Thermal efficiency η_T plotted against compressor pressure ratio π_c for all heat exchanger configurations.

4.1.2 Thrust-Specific Fuel Consumption

Thrust-specific fuel consumption S is another primary performance characteristic. The same method of analysis for examining efficiency has been performed for fuel consumption here in Figures 4.5 and 4.6.

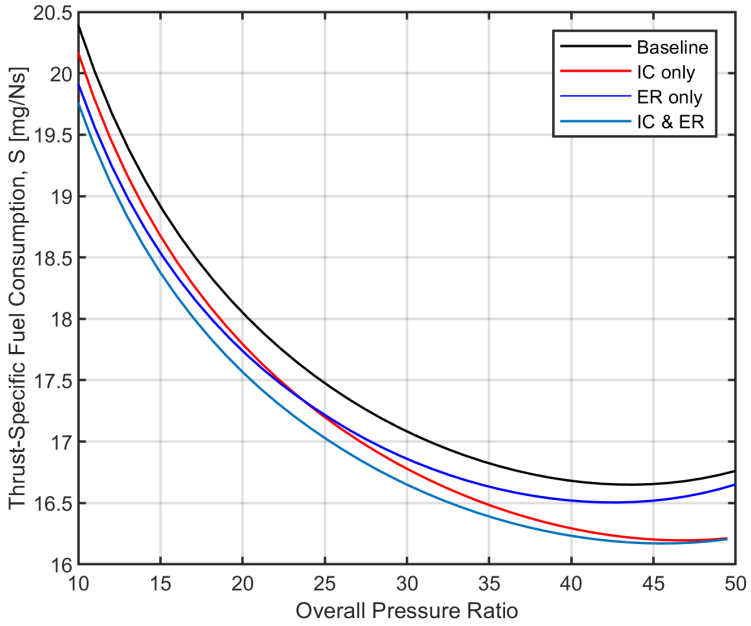

Figure 4.5: Thrust-specific fuel consumption S plotted against compressor pressure ratio π_c for all heat exchanger configurations.

Every configuration provides some benefit to thrust-specific fuel consumption across all overall pressure ratios. The universal benefit can be explained by increasing the available energy from preheating the fuel. Unlike for overall efficiency, the configuration with both intercooling and exhaust recovery (teal line) offers the greatest benefit for fuel consumption. By examining Figure 4.6, it can be seen that exhaust recovery offers greater benefit at lower overall pressure ratios while intercooling does so for higher pressure ratios. The system with both appears to compound these benefits, offering high fuel consumption reduction across all pressure ratios.

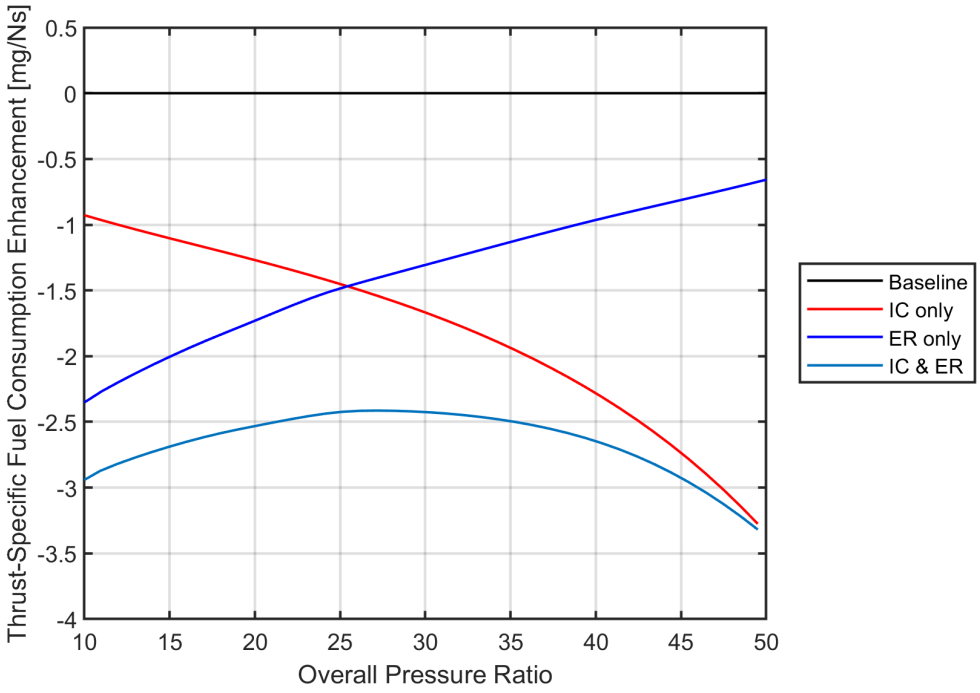

Figure 4.6: Percentage change in thrust-specific fuel consumption S plotted against compressor pressure ratio π_c for all heat exchanger configurations.

4.2 Effects of Major Design Parameters

The following section is a discussion on results featuring the effect of different parameters on the overall system performance.

4.2.1 Effect of Heat Exchanger Effectiveness

For the initial performance analysis, it was assumed that all heat exchangers are designed with a high effectiveness of $\varepsilon = 0.8$. This value could potentially be impractical in some cases due to design limitations of the heat exchanger. Thus, it is important to look at the effect of heat exchanger effectiveness on the major performance characteristics. Based on the results presented in Figures 4.7 and 4.8, higher effectivenesses are desirable and only serve to benefit overall efficiency and fuel consumption for configurations with intercooling (red and teal lines). For just exhaust recovery alone (blue line) however, higher effectiveness actually increases the penalty to overall efficiency, but it still increases benefits to thrust-specific fuel consumption.

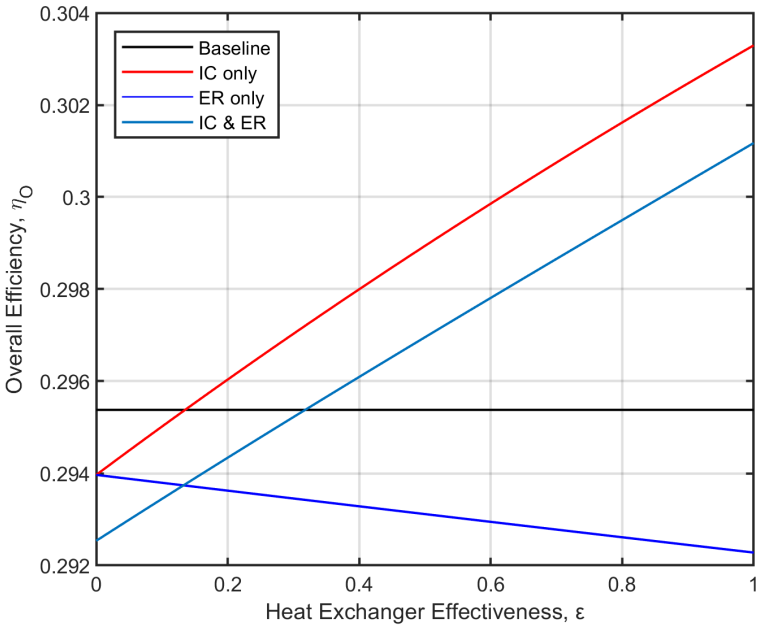

Figure 4.7: Overall efficiency η_O plotted as a function of heat exchanger effectiveness ε for all heat exchangers.

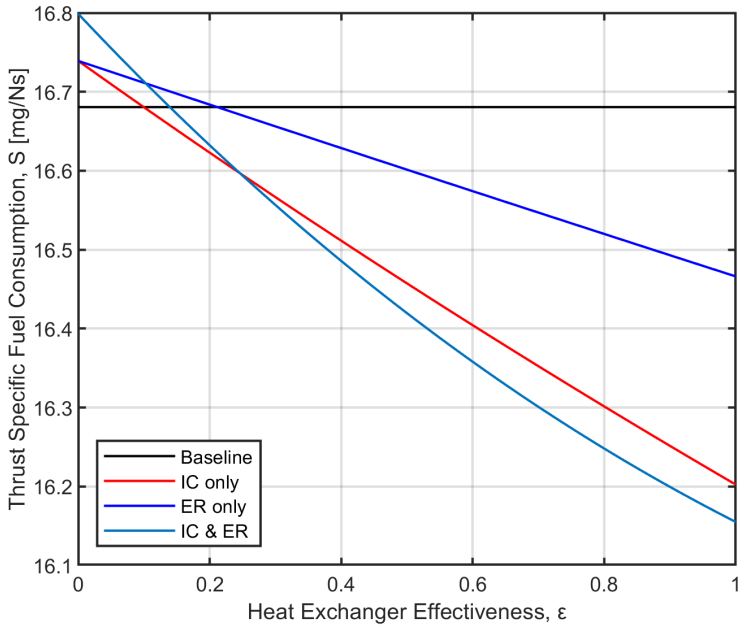

Figure 4.8: Thrust-specific fuel consumption S plotted as a function of heat exchanger effectiveness ε for all heat exchangers.

Figure 4.7 also provides practical limits for the system. An intercooler-only system

fails to enhance overall efficiency if an effectivenesses of over 12% can't be achieved. A system with both intercooling and exhaust recovery fails to enhance overall efficiency if an effectiveness of over 32% can't be achieved. It is important to understand that this cutoff changes if any of the major design parameters change. As such, the interaction between these heat exchanger design parameters are explored further in Section 4.4.

4.2.2 Effect of Heat Exchanger Pressure Drop

The analysis up to this point has assumed a 1% pressure drop for the main flow across each heat exchanger. Much like heat exchanger effectiveness, if the pressure drop across the heat exchanger is too high, then the benefits offered by the system might be nullified due to the pressure losses. This trend is illustrated in Figures 4.9 and 4.10. For a full-system configuration, this occurs at 2.5%. A system with just an intercooler is more forgiving, with the cutoff at around 5.6%. Note that these cutoffs are for overall efficiency, since the cutoff for fuel consumption occurs at a higher pressure drop where efficiency would already incur a major penalty.

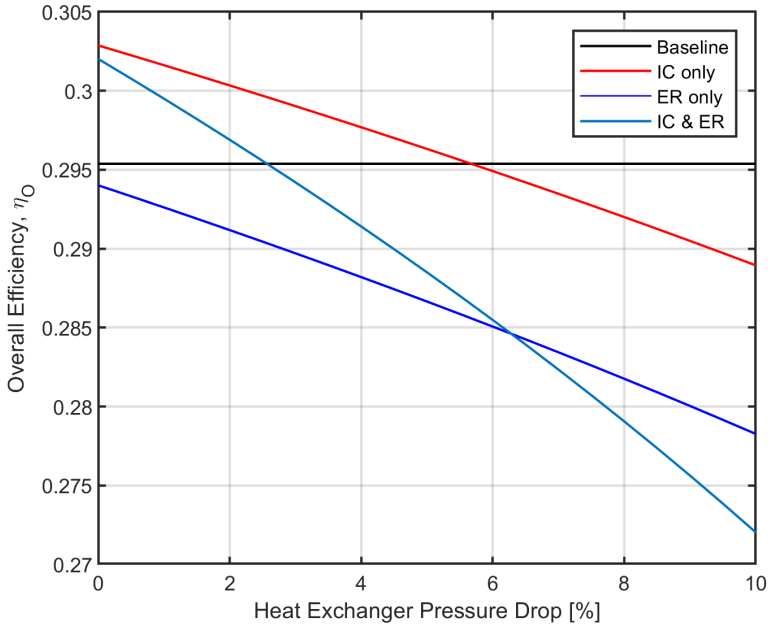

Figure 4.9: Effect of heat exchanger percent pressure drop on overall system efficiency η_O.

Not illustrated in Figure 4.9 is a sharp drop in system efficiency at a pressure drop

of 42% for intercooling only, 36% for exhaust recovery only, and 23% for both combined. Note that this cutoff illustrates a functional limitation of the system. Beyond this point, not only is the system no longer beneficial but altogether inviable as the turbine fails to overcome the pressure losses. Although generally more beneficial, this cutoff occurs earliest for a system with both heat exchangers as incurs pressure loss penalties twice as opposed to once for the systems with just one. This also explains why the rate at which the efficiency decreases and fuel consumption increases is twice that for the double heat exchanger system versus the single heat exchanger systems.

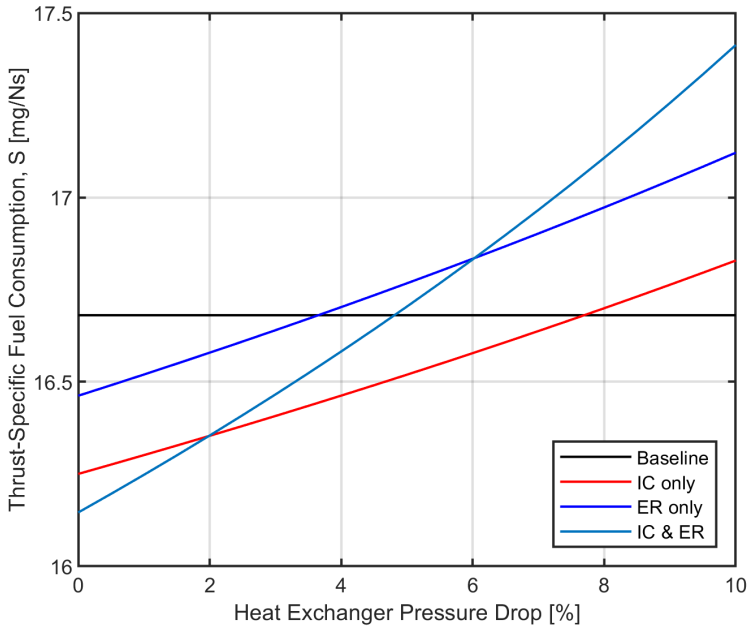

Figure 4.10: Effect of heat exchanger percent pressure drop on thrust-specific fuel consumption S.

4.2.3 Effect of Initial Fuel Temperature

Initial fuel temperature can be expected to have an effect on the overall efficiency of the system, dictating the baseline enthalpy of the fuel. If the fuel starts at a higher temperature, the total heat capacity of the fuel is reduced. Although the results here in Figure 4.11 show that the efficiency drops with an increasing initial fuel temperature, this drop is not pronounced enough even at reasonably elevated temperatures of 0°C to pose detrimental effects to the system.

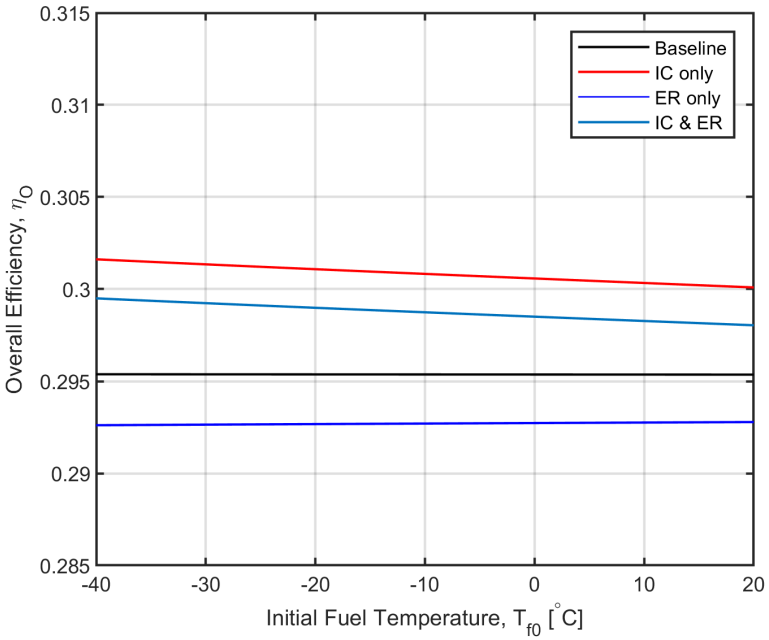

Figure 4.11: Effect of initial fuel temperature T_{f0} on overall system efficiency η_O.

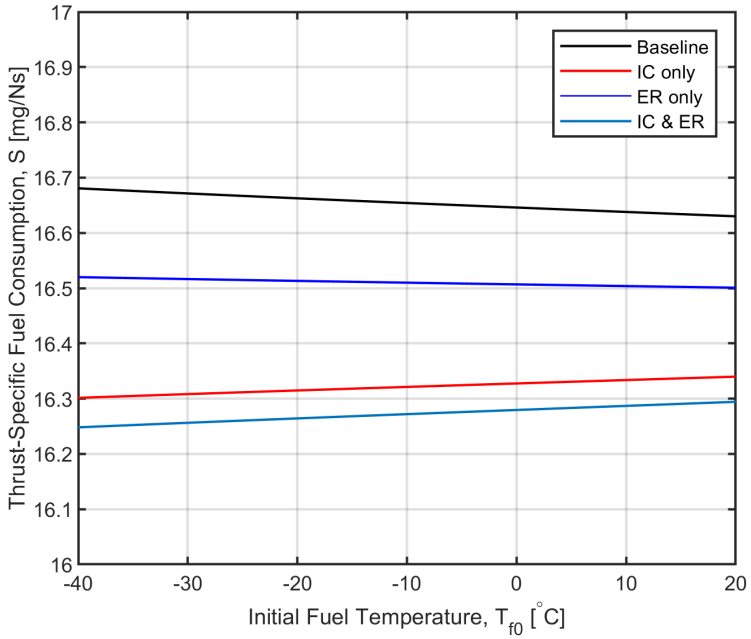

Figure 4.12: Effect of initial fuel temperature T_{f0} on thrust-specific fuel consumption S.

This can be explained by the fuel being heated to much higher temperatures – near 600K in optimal cases. This is true for fuel consumption as well, as shown in Figure

4.12. This indicates that this system can be used alongside traditional fuel storage and management methods without much modification, as elevated initial temperatures do not heavily impact the potential performance enhancement.

4.2.4 Effect of Turbine Inlet Temperature

The temperature of the main flow as it enters the turbine is of critical concern for any gas turbine design. Presented here in Figures 4.13 and 4.14 is performance as a function of practical turbine inlet temperatures.

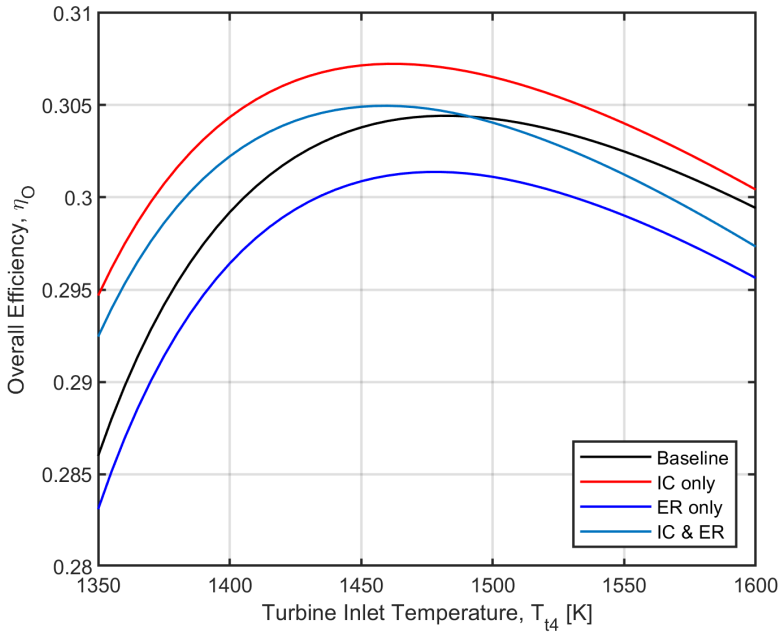

Figure 4.13: Effect of turbine inlet temperature T_{t4} on overall system efficiency η_O.

It should be noted that the figures here do not present a system which is optimized for each value of turbine inlet temperature but instead substitute that value into a system which is optimized for baseline values. This may present a misleading result since it is possible that higher efficiencies would be achieved at increased turbine inlet temperatures if pressure ratios and bypass ratios were adjusted.

Regardless of this deficiency, some major conclusions can still be drawn from the given results. For a given set of input parameters, a system's maximum efficiency and minimum fuel consumption can be achieved at lower turbine inlet temperatures with the

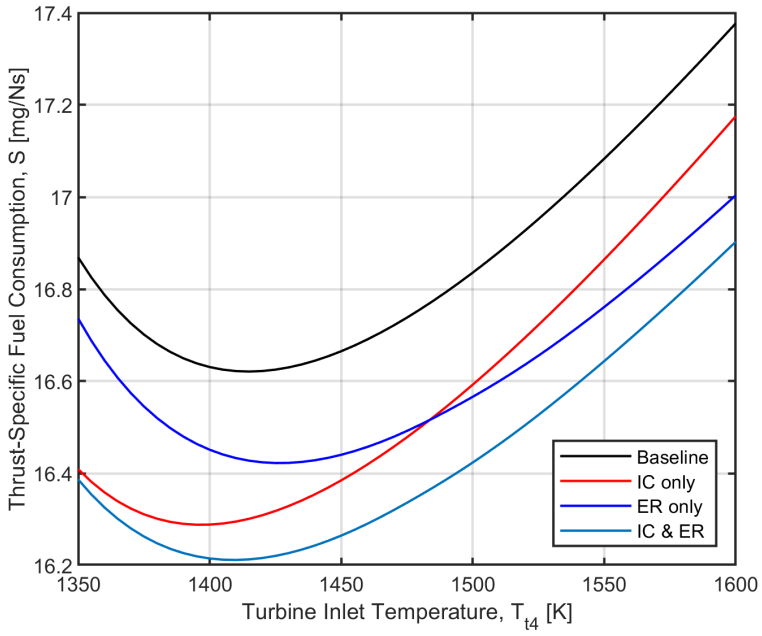

Figure 4.14: Effect of turbine inlet temperature T_{t4} on thrust-specific fuel consumption S.

inclusion of heat exchangers. Minimizing these temperatures essentially means reducing combustion temperatures, which can have other benefits including a decrease in NO_x production. Additionally, the turbine inlet temperature at which the system has the highest overall efficiency is not the same as that for thrust-specific fuel consumption. As such, simultaneously optimizing for both fuel consumption and efficiency using combustion temperatures can not be done. However, the peaks do occur close to one another so there exists a beneficial range at which both low thrust-specific fuel consumption and high overall efficiency can be achieved.

4.3 Recommended Configurations

Based on these performance trends, two out of three configurations have been selected for recommendation – one utilizing both heat exchangers and the other with just the intercooler. It is assumed here that a high heat exchanger effectiveness of $\varepsilon = 0.8$ is achievable.

4.3.1 Full-System Configuration

Presented first is a full-system configuration with all both heat exchangers. This configuration was shown to have the lowest thrust-specific fuel consumption and second highest overall efficiency for high overall pressure ratios. The temperature-entropy diagram for this system is shown here in Figure 4.15. Note the drop in entropy and temperature across each heat exchanger.

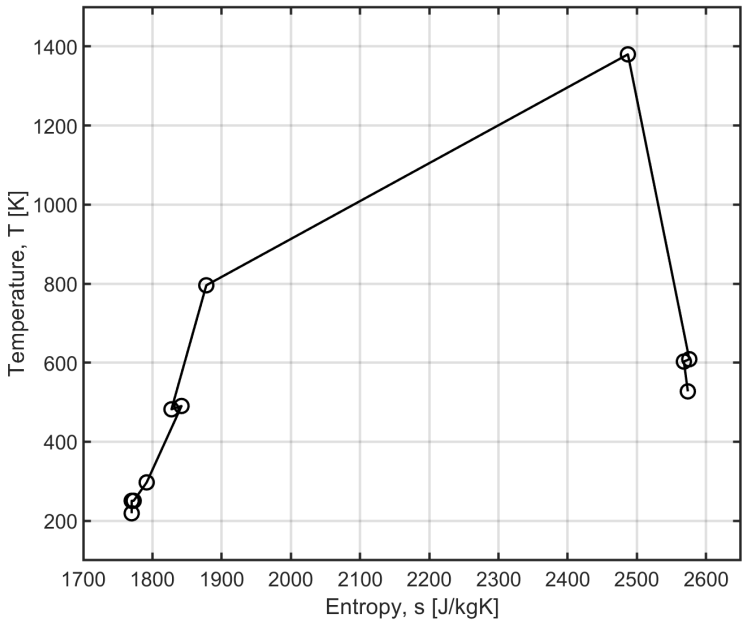

Figure 4.15: The temperature-entropy (T-s) diagram for the full-system configuration (IC & ER).

This diagram illustrates the state of the core flow but does not show changes to the fuel as it passes through the system. Table 4.1 shows the fuel temperature at all stages.

Table 4.1: Fuel temperatures at each stage of the full-system configuration (IC & ER).

Station	$f0$	$f1$	$f2$
T_f [K]	235.2	443.9	578.7

The final performance characteristics of the flow are shown here in Table 4.2. As mentioned earlier,

Table 4.2: Major performance characteristics for the full-system configuration (IC & ER).

Term	Value	Baseline	Difference	Percent Change
$F/\dot{m}$ [J/kg]	139.15	135.69	+3.46	+2.55%
S [mg/Ns]	16.24	16.68	−0.44	−2.62%
η_T	0.3695	0.3610	+0.0085	+2.35%
η_P	0.8109	0.8182	−0.0073	−0.89%
η_O	0.2996	0.2954	+0.0042	+1.44%

4.3.2 Intercooler Only

The second configuration presented here has only one heat exchanger – the intercooler. This configuration was shown previously to yield higher overall efficiencies at the cost of higher thrust-specific fuel consumption. Illustrated here in Figure 4.16 is the T-s diagram for this configuration.

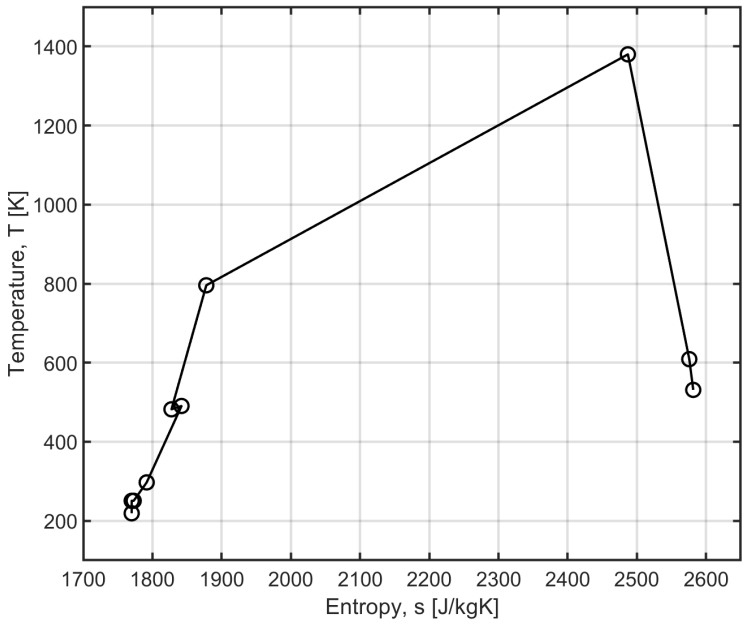

Figure 4.16: The temperature-entropy (T-s) diagram for the intercooler-only configuration (IC).

Here in Table 4.3 are fuel temperatures through the system. Note that there is no change across stations $f1$ and $f2$ due to the lack of exhaust recovery.

Table 4.3: Fuel temperatures at each stage of the intercooler-only configuration (IC).

Station	$f0$	$f1$	$f2$
T_f [K]	235.2	443.9	443.9

The final performance characteristics of the system are shown here in Table 4.4.

Table 4.4: Major performance characteristics of the intercooler-only configuration (IC).

Term	Value	Baseline	Difference	Percent Change
$F/\dot{m}$ [J/kg]	139.15	135.69	+4.25	+3.14%
S [mg/Ns]	16.30	16.68	−0.38	−2.27%
η_T	0.3728	0.3610	+0.0117	+3.25%
η_P	0.8091	0.8182	−0.0090	−1.10%
η_O	0.3016	0.2954	+0.0062	+2.11%

4.4 Heat Exchanger Design

Presented here are the heat exchanger design parameters pressure drop and effectiveness with their respective effects on performance. The same color maps are used across the same performance parameters, so colors refer to the same value across figures for both configurations. The specialized divergent color maps are based on ColorBrewer, by Cynthia A. Brewer [27]. For Figures 4.17 to 4.22, beneficial regions are blue while detrimental regions are red. The white region indicates that values are close to zero. Black lines correspond to the labeled marks on the colorbar – either increments of 0.5 or 1 depending on the figure. Note that the line through the middle in the white region represents the point at which the configuration has no comparable effect on the given parameter over the baseline. The region under this line is then the design space where the technology is predicted to be beneficial.

In Figures 4.17 and 4.18 are the overall efficiency of the systems, plotted as a function of heat exchanger design parameters. Like previous figures comparing efficiency in this section, these figures portray a difference in efficiencies rather than a percent change.

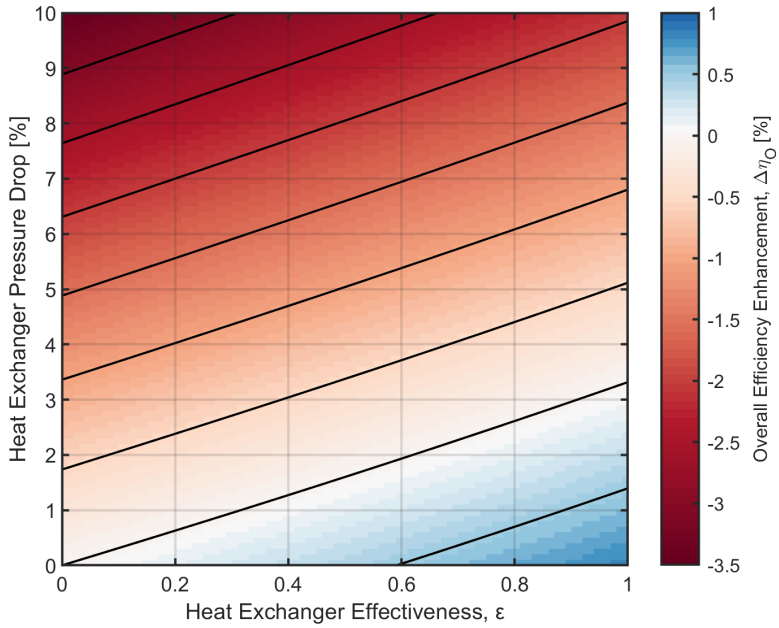

Figure 4.17: The effects of heat exchanger design parameters on overall efficiency enhancement for full-system configuration (IC & ER).

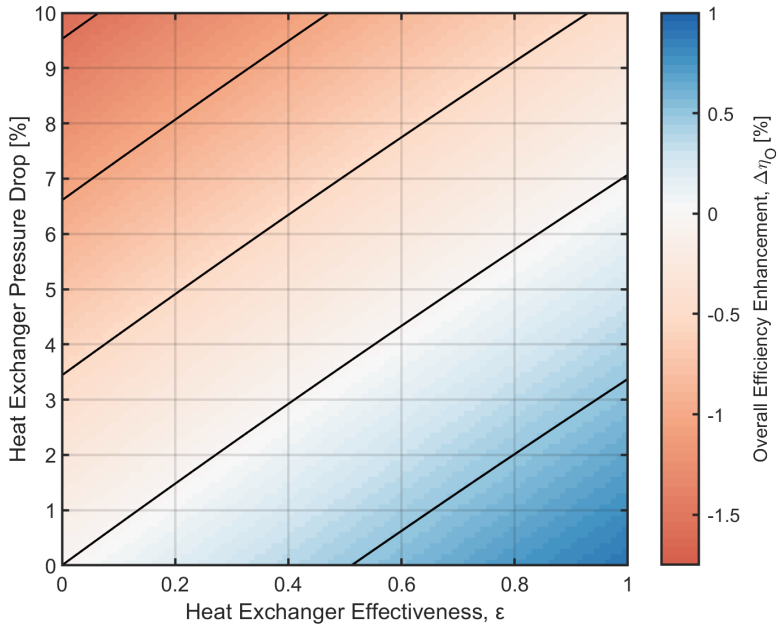

Figure 4.18: The effects of heat exchanger design parameters on overall efficiency enhancement for intercooler-only configuration (IC).

As shown with the fixed-parameter analysis previously, the intercooler-only configu-

ration offers slightly better efficiency enhancement.

The intercooler-only configuration is also more forgiving than the full-system configuration when it comes to efficiency, having smaller performance penalties as a function of pressure drop. This is due to the full-system configuration receiving the pressure drop penalty twice – once for both heat exchangers. This trend carries through for all the major performance parameters.

Figures 4.19 and 4.20 illustrate the effects on thrust-specific fuel consumption. Unlike figures presented previously comparing thrust-specific fuel consumption, this value for enhancement is a percent change rather than a difference. The range of beneficial parameters is much larger for fuel consumption than for efficiency, a result which could be expected based on the initial comparison in Figure 4.5. Even a slight amount of fuel preheat increases fuel enthalpy enough to overcome large pressure drops.

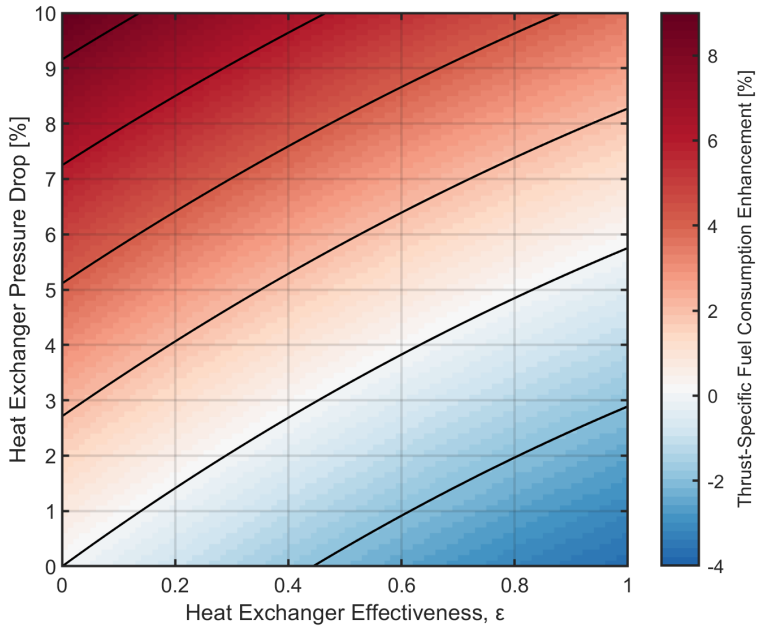

Figure 4.19: The effects of heat exchanger design parameters on thrust-specific fuel consumption enhancement for full-system configuration (IC & ER).

As shown previously, the full-system configuration achieves the greatest reductions in thrust-specific fuel consumption – close to 4% in the most optimal scenario. This is due to the higher temperature preheat of the exhaust recovery. However, this comes at the cost

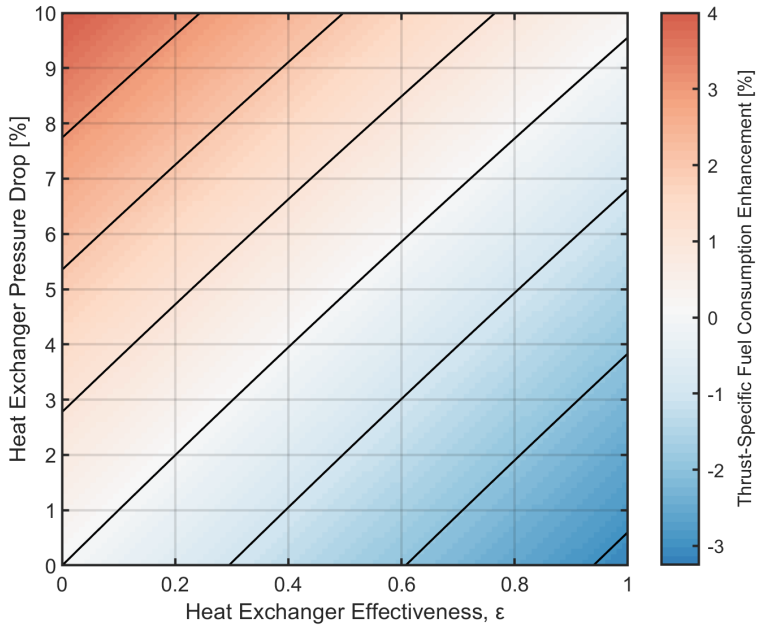

Figure 4.20: The effects of heat exchanger design parameters on thrust-specific fuel consumption enhancement for intercooler-only configuration (IC).

of an additional heat exchanger which doubles the performance penalties from pressure drop, as was the case with efficiency as well.

Lastly, Figures 4.21 and 4.22 show the thermal efficiency of these two configurations as a function of heat exchanger design. To restate from before, the driving factor behind the overall efficiency enhancement is the thermal efficiency. Following this trend, the thermal efficiency enhancement is overall much higher than the overall efficiency enhancement. With the compressor heat exchangers, the most favorable condition exhibits a greater than 1.75% improvement compared to the 1% improvement in overall efficiency for the same conditions. Additionally, the greatest detrimental effects in this range are far lower for thermal efficiency. Despite this, the neutral effect line (i.e., 0% line, white region) occurs in approximately the same region as that for overall efficiency.

Overall efficiency appears to be the most limiting performance characteristic, featuring the smallest acceptable (blue) region. As such, these figures (Figures 4.17 and 4.18) should be used for reference when designing heat exchangers for this application in future work.

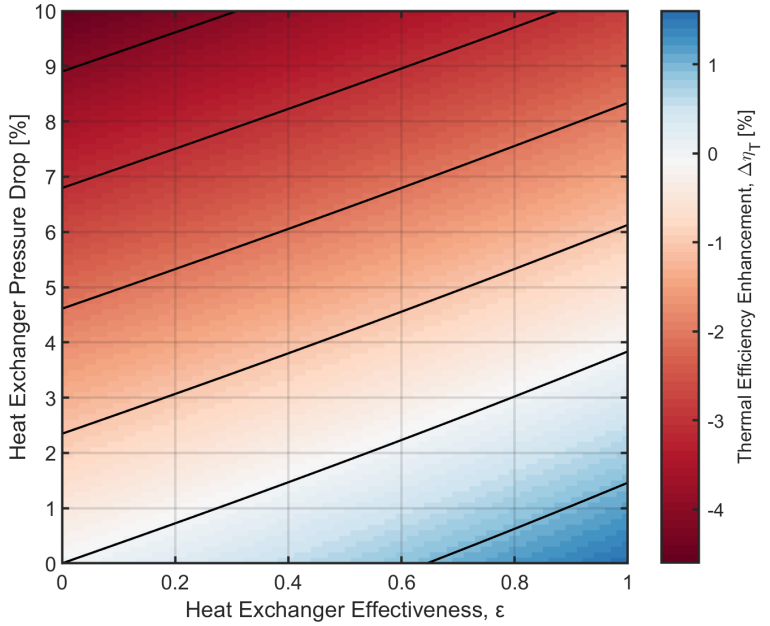

Figure 4.21: The effects of heat exchanger design parameters on thermal efficiency enhancement for full-system configuration (IC & ER).

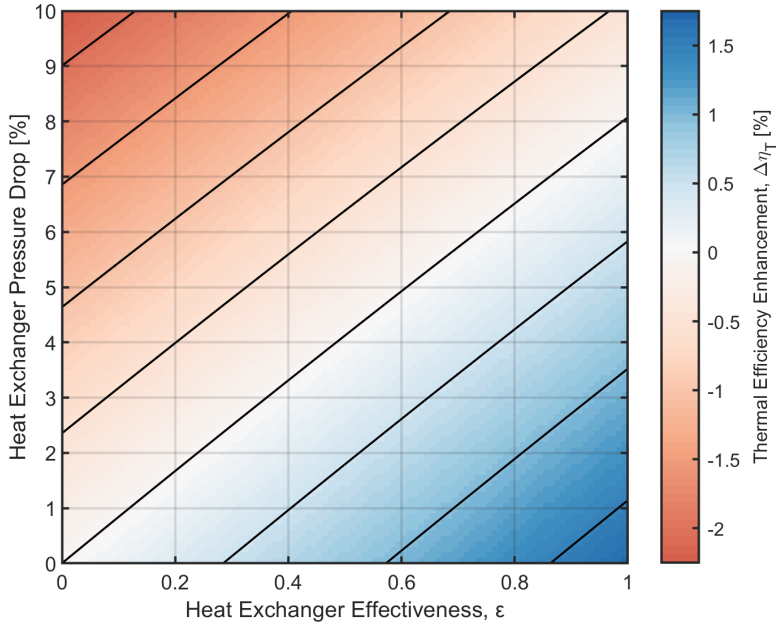

Figure 4.22: The effects of heat exchanger design parameters on thermal efficiency enhancement for intercooler-only configuration (IC).

Chapter 5

Conclusion

5.1 Major Conclusions

Based on the results of this study, the system proposed here shows promise as a way to enhance the performance of existing turbofan engines. Both recommended configurations offer significant benefits over the baseline case. Raw values for performance characteristics are less important results than the improvements over the baseline case. The overall enhancement that the system provides offers insight as to how the technology could benefit existing engines.

It was determined that a full-system configuration could provide a wide range of performance benefits. This preliminary analysis of the system shows a 2.55% increase in specific thrust, a 2.62% reduction in thrust-specific fuel consumption, a 1.44% increase in overall efficiency, and a 2.35% increase in thermal efficiency.

Utilizing only the intercooler, most of these benefits extend further at the cost of a smaller reduction in fuel consumption. The same analysis showed that the system could yield a 3.14% increase in specific thrust, a 2.27% reduction in thrust-specific fuel consumption, a 2.11% increase in overall efficiency, and a 3.25% increase in thermal efficiency. This system also receives half the performance penalties that come from increased pressure drop across the heat exchangers as it only has one heat exchanger. This would be preferred over the full system configuration if large pressure drops are unavoidable.

An important result from this work was the identification of practical limitations. It

was determined that the technology is only beneficial if a heat exchanger effectiveness greater than 32% and a heat exchanger pressure drop less than 2.5% are achievable. A specific design space for the heat exchangers was also identified for beneficial results of both primary configurations as well. Within these limits, the technology should be beneficial for a wide range of cases.

5.2 Recommendations for Future Work

Since this work only presents a preliminary analysis, much work is required to bring this concept to a fully detailed design.

First, a more detailed and accurate analysis of the system can be conducted with variable specific heats over every component would be of value. One of the primary assumptions limiting the accuracy of the analysis is the assumption of constant specific heats for the core flow before and after the combustor. The inclusion of variable specific heats would allow for a more detailed and accurate performance analysis.

A detailed heat exchanger design should be made now that practical limitations have been set. Without specifications for the heat exchanger, a reasonable sizing analysis cannot be made. A degradation analysis and study of possible carbon deposition over operational lifetime should be conducted as part of the heat exchanger design. Coking is an inevitable problem for any system working with hydrocarbon fuels at high temperatures. Different implementations of heat exchangers should also be explored. Possibilities include heat exchangers integrated directly into existing components like the stators of the compressor and turbine or independent co-flow heat exchangers.

After the heat exchangers are designed, a basic 2D and 3D render can be made, fully visualizing component structure and interactions. After the full models of the system are developed, running 2D and 3D flow simulations would be necessary to provide more realistic values for system performance characteristics. These flow simulations will require a detailed characterization of fuel properties across a wide range of temperatures, for both heat capacities as well as combustion characteristics. This characterization may not exist yet within the literature and should be examined as well.

Appendix A

Code Listing

A.1 Base Code

As follows is the base code used. Additional loops were necessary to produce plots although the main structure was not change. This version of the code has been commented for flexibility in future use. Other codes used for plotting can be accessed by contacting the author.

Note that the subscript of station numbers with decimal places have these decimal places removed based on restrictions of MATLAB variable names (e.g 2.1 to 21).

```
% Fuel-Integrated Energy Recuperation Aeroengine (FIERA) Model
% Steven Wong
% UC Davis MAE
% v3

% Core code. Compares to baseline and plots T-s diagram.

close all
clear
clc

M_0 = 0.85;      %inlet mach number [-]
```

```
13 T_0 = 218.934;  %inlet temperature [K]
14 P_0 = 23.9;     %inlet pressure [kPa]
15 gamma_c = 1.4;  %[-]
16 c_pc = 1004;    %[J/kgK]
17 gamma_t = 1.35; %[-]
18 c_pt =  1096;  %[J/kgK]
19
20 pi_d = 0.99;     %inlet pressure ratio
21 pi_b = 0.98;     %burner pressure ratio
22 pi_f = 1.7;      %fan pressure ratio
23 pi_n = 0.98;     %nozzle pressure ratio
24 pi_fn = 0.99;    %fan nozzle pressure ratio
25 pi_lpc = 4.85;  %lpc pressure ratio
26 pi_hpc = 4.85;  %hpc presure ratio
27 e_c = 0.90;      %compressor polytropic efficiency
28 e_f = 0.89;      %fan polytropic efficiency
29 e_t = 0.91;      %turbine polytropic efficiency
30 eta_n = 0.98;    %nozzle efficiency
31 eta_b = 0.99;    %burner efficiency
32 eta_m = 0.99;    %mechanical efficiency
33 alpha = 6.5;     %bypass ratio
34 P0P9 = 0.9;
35 P0P19 = 0.9;
36 TIT = 1380;
37 g_c = 1;
38
39 % Heat Exchanger Terms
40 load('jp8.mat') %loads jp8ht, jp8th functions
41 eps_IC = [0  0.8];
```

```
42 eps_ER = [0  0.8];
43
44 pi_IC = [1  0.99];  %intercooling
45 pi_ER = [1  0.99];  %exhaust recovery
46
47 T_f0 = 273.15-40;   %-47 is freezing
48 h_pr_ref = 4.33e7;   %[J/kg]
49 m = 2;
50
51 % Preallocate
52 Fmdot = zeros(1,m);
53 S = zeros(1,m);
54 S_mg = zeros(1,m);
55 eta_T = zeros(1,m);
56 eta_P = zeros(1,m);
57 eta_O = zeros(1,m);
58
59 % Initial Guess
60 f = 0.02;   %kg/kg
61
62 for i=1:m
63
64 %% Stages 0-3
65
66 % Coefficients
67 R_c = (gamma_c-1)*c_pc/gamma_c;
68 R_t = (gamma_t-1)*c_pt/gamma_t;
69
70 % Inlet
```

```
71 a_0 = sqrt(gamma_c*R_c*g_c*T_0);
72 V_0 = a_0*M_0;
73
74 T_t0 = T_0*(1+0.5*(gamma_c-1)*(M_0^2));
75 P_t0 = P_0*(1+0.5*(gamma_c-1)*(M_0^2))^(gamma_c/(gamma_c-1));
76 T_t2 = T_t0;
77 P_t2 = P_t0*pi_d;
78
79 % Fan
80 P_t21 = P_t2*pi_f;
81 T_t21 = T_t2*(pi_f^((gamma_c-1)/(gamma_c*e_f)));
82
83 % Low Pressure Compressor (LPC)
84 P_t25 = P_t21*pi_lpc;
85 T_t25 = T_t21*(pi_lpc^((gamma_c-1)/(gamma_c*e_c)));
86
87 % f Loop
88 f_new = 0;
89 dx = abs(f_new-f);
90
91 while dx>0.001
92 % Intercooler (HX1)
93 P_t26 = P_t25*pi_IC(i);
94 h_f0 = h_f(T_f0);
95 T_t26 = T_t25-(eps_IC(i)*f/c_pc)*(h_f(T_t25)-h_f0);
96 h_f1 = h_f0+(c_pc/f)*(T_t25-T_t26);
97
98 % High Pressure Compressor (HPC)
99 P_t3 = P_t26*pi_hpc;
```

```
100 T_t3 = T_t26*(pi_hpc^((gamma_c-1)/(gamma_c*e_c)));
101
102 %% Stages 4-5 Baseline
103 % Combustor
104 P_t4 = P_t3*pi_b;
105 T_t4 = TIT;
106 h_pr = h_pr_ref;
107 f = (c_pt*T_t4-c_pc*T_t3)/(eta_b*h_pr-c_pt*T_t4);
108 % Turbine
109 T_t5 = T_t4*(1-((c_pc*T_t0)/(eta_m*(1+f)*c_pt*T_t4))*((T_t3/T_t2
        )-1+alpha*((T_t21/T_t2)-1)));
110
111 %% Stages 31-5 Iterative
112 T_t5_new = 0;
113 dy = abs(T_t5_new-T_t5);
114
115 while dy > 0.0001
116
117 % Exhaust Recovery (HX2)
118 h_f2 = eps_ER(i)*(h_f(T_t5)-h_f1)+h_f1;
119
120 % Combustor
121 P_t4 = pi_b*P_t3;
122 T_t4 = TIT;
123 h_pr = h_pr_ref+h_f2;
124 f_new = (c_pt*T_t4-c_pc*T_t3)/(eta_b*h_pr-c_pt*T_t4);
125
126 % Turbine
127 T_t5_new = T_t4*(1-((c_pc*T_t0)/(eta_m*(1+f_new)*c_pt*T_t4))*((
```

```
    T_t3/T_t2)-1+alpha*((T_t21/T_t2)-1)));

dy = abs(T_t5_new-T_t5);
T_t5 = T_t5_new;
end

dx = abs(f_new-f);
f = f_new;
end

%% Stages 5-9
% Turbine
P_t5 = P_t4*(T_t5/T_t4)^(gamma_t/((gamma_t-1)*e_t));

% Exhaust Recovery (HX2)
T_t51 = T_t5-(eps_ER(i)*f/(c_pt*(1+f)))*(h_f(T_t5)-h_f1);
P_t51 = P_t5*pi_ER(i);

% Nozzle
P_t9 = P_t51*pi_n;
P_9 = P_0/P0P9;
M_9 = sqrt((2/(gamma_t-1))*((P_t9/P_9)^((gamma_t-1)/(gamma_t))
    -1));
T_9 = T_t51*(P_t9/P_9)^((1-gamma_t)/gamma_t);
T9T0 = T_9/T_0;
V9a0 = M_9*sqrt((gamma_t*R_t*T9T0)/(gamma_c*R_c));

% Fan Nozzle
P_t19 = P_t21*pi_fn;
```

```
155 P_19 = P_0/P0P19;
156 M_19 = sqrt((2/(gamma_c-1))*((P_t19/P_19)^((gamma_c-1)/(gamma_c)
        )-1));
157 T_19 = T_t21*(P_t19/P_19)^((1-gamma_c)/gamma_c);
158 T19T0 = T_19/T_0;
159 V19a0 = M_19*sqrt(T19T0);
160
161 %% Final Performance
162 Fmdot(i) = (1/(1+alpha))*(a_0/g_c)*((1+f)*V9a0-M_0+(1+f)*((R_t*
        T9T0)/(R_c*V9a0))*(1-P0P9)/gamma_c)+(alpha/(1+alpha))*(a_0/
        g_c)*(V19a0-M_0+(T19T0/V19a0)*(1-P0P19)/gamma_c);
163 S(i) = f/((1+alpha)*Fmdot(i));
164 S_mg(i) = S(i)*1e6;
165 eta_T(i) = a_0^2*((1+f)*(V9a0)^2+alpha*(V19a0)^2-(1+alpha)*M_0
        ^2)/(2*g_c*f*h_pr);
166 eta_P(i) = 2*M_0*((1+f)*V9a0+alpha*V19a0-(1+alpha)*M_0)/((1+f)*
        V9a0^2+alpha*V19a0^2-(1+alpha)*M_0^2);
167 eta_O(i) = eta_P(i)*eta_T(i);
168 % FR = ((1+f)*V9a0-M_0+(1+f)*(((R_t*T9T0)/(R_c*V9a0))*((1-P0P9)/
        gamma_c)))/(V19a0-M_0+(T19T0/V19a0)*((1-P0P19)/gamma_c))
169 end
170
171 mdot = 802;
172 F = Fmdot*mdot/1000;
173
174 %% Percent Change
175 pcnt = @(x) 100*(x(2)-x(1))/x(1);
176 diff = @(x) x(2)-x(1);
177
```

```
178 %% T-s Plotting
179 T_all = [T_0 T_t0 T_t2 T_t21 T_t25 T_t26 T_t3 T_t4 T_t5 T_t51
      T_9];
180 P_all = [P_0 P_t0 P_t2 P_t21 P_t25 P_t26 P_t3 P_t4 P_t5 P_t51
      P_9];
181 s_all = zeros(1,11);
182 s_all(1) = 1770;
183 figure(1)
184 hold on
185 for i=1:6
186     s_all(i+1) = s_all(i)+c_pc*log(T_all(i+1)/T_all(i))-R_c*log(
        P_all(i+1)/P_all(i));
187 end
188 for i=7:10
189     s_all(i+1) = s_all(i)+c_pt*log(T_all(i+1)/T_all(i))-R_t*log(
        P_all(i+1)/P_all(i));
190 end
191 plot(s_all,T_all,'ko-')
192 xlabel('Entropy, s [J/kgK]')
193 ylabel('Temperature, T [K]')
194 axis([1700 2650 100 1500])
195 grid on
196 box on
```

References

[1] Environmental Protection Agency, "EPA Determines that Aircraft Emissions Contribute to Climate Change Endangering Public Health and the Environment," Jul 2016.

[2] Federal Aviation Administration, "Continuous Lower Energy, Emissions, and Noise (CLEEN) Program," Mar 2018.

[3] Mattingly, J. D. and Ohain, H. V., *Elements of Gas Turbine Propulsion*, AIAA Education Series, AIAA, 2005.

[4] El-Sayed, A. F., *Aircraft Propulsion and Gas Turbine Engines*, CRC Press, 2008.

[5] Pasini, S., Ghezzi, I., Andriani, R., and Ferri, L., "Heat Recovery from Aircraft Engines," *35th Intersociety Energy Conversion Engineering Conference and Exhibit*, Vol. 1, IEEE, 2000, pp. 546–553.

[6] Han, J.-C., "Fundamental Gas Turbine Heat Transfer," *Journal of Thermal Science and Engineering Applications*, Vol. 5, No. 2, 2013, pp. 021007.

[7] Han, J.-C. and Rallabandi, A., "Turbine Blade Film Cooling Using PSP Technique," *Frontiers in Heat and Mass Transfer (FHMT)*, Vol. 1, No. 1, 2010.

[8] Fu, W.-L., Wright, L. M., and Han, J.-C., "Rotational Buoyancy Effects on Heat Transfer in Five Different Aspect-Ratio Rectangular Channels With Smooth Walls and 45 Degree Ribbed Walls," *Journal of Heat Transfer*, Vol. 128, No. 11, Apr 2006, pp. 1130–1141.

[9] Lander, H. and Nixon, A., "Endothermic Fuels for Hypersonic Vehicles," *Journal of Aircraft*, Vol. 8, No. 4, Apr 1971, pp. 200–207.

[10] Puri, P., Ma, F., Choi, J.-Y., and Yang, V., "Ignition Characteristics of Cracked JP-7 Fuel," *Combustion and Flame*, Vol. 142, No. 4, Sep 2005, pp. 454–457.

[11] Harrison, W. E., Binns, K. E., Anderson, S. D., and Morris, R. W., "High Heat Sink Fuels for Improved Aircraft Thermal Management," *International Conference On Environmental Systems*, SAE International, Jul 1993.

[12] Huang, H., Spadaccini, L. J., and Sobel, D. R., "Fuel-Cooled Thermal Management for Advanced Aeroengines," *Journal of Engineering for Gas Turbines and Power*, Vol. 126, No. 2, 2004, pp. 284–293.

[13] Wickham, D. T., Engel, J. R., Rooney, S., and Hitch, B. D., "Additives to Improve Fuel Heat Sink Capacity in Air/Fuel Heat Exchangers," *Journal of Propulsion and Power*, Vol. 24, No. 1, 2008, pp. 55–63.

[14] Crisalli, A. J. and Parker, M. L., "Overview of the WR-21 Intercooled Recuperated Gas Turbine Engine System: A Modern Engine for a Modern Fleet," *ASME 1993 International Gas Turbine and Aeroengine Congress and Exposition*, No. 93-GT-231, ASME, 1993, p. V03AT15A082.

[15] Boggia, S. and Rüd, K., "Intercooled Recuperated Gas Turbine Engine Concept," *41st AIAA/ASME/SAE/ASEE Joint Propulsion Conference & Exhibit*, AIAA, Jul 2005, p. 4192.

[16] Kyprianidis, K. G., Grönstedt, T., Ogaji, S. O., Pilidis, P., and Singh, R., "Assessment of Future Aero-engine Designs With Intercooled and Intercooled Recuperated Cores," *Journal of Engineering for Gas Turbines and Power*, Vol. 133, No. 1, Sep 2011, pp. 011701.

[17] Kormann, M. and Schaber, R., "An Intercooled Recuperative Aero Engine for Regional Jets," *ASME Turbo Expo 2014: Turbine Technical Conference and Exposition*, American Society of Mechanical Engineers, 2014, pp. V03AT07A021–V03AT07A021.

[18] Zhao, X., Thulin, O., and Grönstedt, T., "First and Second Law Analysis of Intercooled Turbofan Engine," *Journal of Engineering for Gas Turbines and Power*, Vol. 138, No. 2, 2016, pp. 021202.

[19] Jacob, F., Rolt, A. M., Sebastiampillai, J. M., Sethi, V., Belmonte, M., and Cobas, P., "Performance of a Supercritical CO2 Bottoming Cycle for Aero Applications," *Applied Sciences*, Vol. 7, No. 3, 2017, pp. 255.

[20] Callas, J. J., "Turbine engine having fuel-cooled air intercooling," Jul 2012, US Patent 8,220,268.

[21] Society of Automotive Engineers, *Gas Turbine Engine Performance Station Identification and Nomenclature, Aerospace Recommended Practice, ARP 755A*, 1974.

[22] Mattingly, J. D., Heiser, W. H., and Pratt, D. T., *Aircraft Engine Design*, AIAA Education Series, AIAA, 2002.

[23] Gray, C. N. and Shayeson, M. W., "Aircraft Fuel Heat Sink Utilization," Tech. Rep. AFAPL-TR-73-51, General Electric Co., July 1973.

[24] Langton, R., Clark, C., Hewitt, M., and Richards, L., *Aircraft Fuel Systems*, Vol. 24 of *Aerospace Series*, John Wileey & Sons, 2009.

[25] Coordinating Research Council, *Handbook of Aviation Fuel Properties*, No. 663 in CRC report, Coordinating Research Council, Incorporated, 2014.

[26] Bergman, T. L. and Incropera, F. P., *Fundamentals of Heat and Mass Transfer*, John Wiley & Sons, 2011.

[27] Brewer, C. A. and Harrower, M., "Color Brewer 2.0," 2012.